Master's thesis

NTNU
Norwegian University of Science and Technology
Faculty of Natural Sciences
Department of Biology

Lise Rønning

Growth and Biochemical Composition of Cultivated Mixed Biofilm on Wastewater from Recirculating Aquaculture Systems (RAS)

Master's thesis in Biotechnology (MBIOT5)
Supervisor: Kjell Inge Reitan
Co-supervisor: Kari Attramadal (Nofitech) and Charlotte Volpe (SINTEF)

June 2023

NTNU
Norwegian University of Science and Technology

Lise Rønning

Growth and Biochemical Composition of Cultivated Mixed Biofilm on Wastewater from Recirculating Aquaculture Systems (RAS)

Master's thesis in Biotechnology (MBIOT5)
Supervisor: Kjell Inge Reitan
Co-supervisor: Kari Attramadal (Nofitech) and Charlotte Volpe (SINTEF)
June 2023

Norwegian University of Science and Technology
Faculty of Natural Sciences
Department of Biology

NTNU
Norwegian University of Science and Technology

Acknowledgements

My master's thesis in Biotechnology marks the end of five amazing years as a student at the Norwegian University of Science and Technology (NTNU). I would like to extend my sincere appreciation to all those who contributed to the successful completion of this research project.

This study was conducted at the Department of Biology (IBI) and was a part of the research project "WASTELESS", which is a collaboration between Nofitech, NTNU and SINTEF. My main supervisor was Kjell Inge Reitan (Professor at the Department of Biology at NTNU), and co-supervisors were Kari Attramadal (Head of R&D at Nofitech) and Charlotte Volpe (Researcher at SINTEF Ocean).

I would like to express my gratitude to my supervisors Kjell Inge and Kari for providing me the opportunity to be a part of this innovative and exciting project. Thank you for always being available to answer questions, offer guidance and share experiences throughout this two-year journey. It has been truly amazing! Secondly, I would like to extend my sincerest gratitude to Hubert Bonnefond (CEO of the DareWin project at Inria). Your support and dedication have been instrumental in the success of this project. I would also like to thank Siv Anina Etter (Department Engineer at NTNU), Zdenka Bartosova (Department Engineer at NTNU) and Merethe Selnes (Senior Engineer at SINTEF) for the help with biochemical analyses, as well as Dag Altin (Senior Engineer at NTNU) for all help during the experimental work. And a big thanks to the WASTELESS Team for the countless Friday meetings and great advice. I have really appreciated to be a part of your research group!

Finally, I would like to thank my fiancé and my cherished family and friends who have shown unwavering understanding during the long days spent in the lab, who have cheered me on and given me lots of love and support throughout these five years! A special thanks goes to Johan, my research partner and close friend. From the countless coffee breaks to the long lab sessions, we have truly laughed our way through everything together!

Trondheim, June 2023

Lise Rønning

Abstract

There has been an increase in the use of Recirculating Aquaculture Systems (RAS) to produce Atlantic salmon smolts (*Salmo salar*). However, concerns have been raised regarding the environmental pollution associated with aquaculture wastewater. RAS water contains substantial amounts of inorganic nitrogen and phosphorous which can impact the local ecosystems. Nitrogen accumulation in RAS can also pose a potential threat to the fish and need to be treated before reaching a toxic level. Meanwhile, nitrogen and phosphorus deficiency pose a global threat, as binding nitrogen from the atmosphere is responsible for 1% of the energy consumption and 1.4% of the CO_2 footprint on a global scale. Also, the "peak phosphorous" theory describes how the world will be depleted of phosphorous within the end of the century, posing a serious threat to the worlds food security.

The present study aimed to address the challenge of nutrient management in RAS. By cultivating the microorganisms present in the RAS water as a mixed community biofilm in a bioreactor, this system can utilize nutrients in the RAS water, thus contributing to the water treatment process. Additionally, the biofilm product can be harvested and utilized as a potential feedstock or fertilizer ingredient due to the valuable biochemical composition associated with microalgal biomass. This study therefore aimed to develop a growth system for this mixed biofilm of microorganisms present in the RAS water from Hardingsmolt AS. Important influencing factors for biofilm development and cultivation was determined. Additionally, the biochemical composition of the biomass produced under different harvest frequencies, was determined, and compared to the biomass obtained in a pilot study on-site at Hardingsmolt AS.

Photoautotrophic organisms were found to dominate the biofilm consortium, indicating light as an important factor for cultivation. Further, the biomass yield and productivity significantly increased with the addition of silica to the RAS water, keeping a high nutrient concentration, and harvesting of the biofilm every 12 days. The biochemical profiles of the biofilm product under the effect of different harvest frequencies (4 days, 8 days, 12 days) were characterized. The 12 day harvest frequency condition had significantly higher values for total protein (363 mg g^{-1} DW), nitrogen, and carbon contents and sum non-essential amino acids (208 mg g^{-1} DW). When the biofilm product obtained in the lab was compared to the one from the on-site pilot reactors, no significant differences was found. The valuable polyunsaturated fatty acids, eicosapentaenoic acid (EPA), and docosahexaenoic acid (DHA) was both present in all groups, where the 12 day harvest frequency had somewhat, but not significantly, higher contents of both DHA and EPA. High levels of palmitoleic acid were also found in all three conditions.

The results obtained in the present study, demonstrated the successful cultivation of mixed community biofilm from RAS water (Hardingsmolt AS), which was recognized as a promising component in both RAS water treatment and as a potential feedstock ingredient.

Sammendrag

Bruken av Resirkulerende akvakultursystemer (RAS) for å produsere atlantisk laksesmolt (Salmo salar) har økt de siste årene. Med økningen har det imidlertid også blitt uttrykt bekymringer angående miljøforurensningen knyttet til avløpsvann fra akvakulturindustrien. RAS vann inneholder betydelige mengder inorganisk nitrogen og fosfor som kan påvirke de lokale økosystemene. Opphopning av nitrogen og fosfor i RAS kan også utgjøre en potensiell trussel mot fisken, og må behandles slik at ikke giftige nivåer nås. Samtidig utgjør nitrogen- og fosfor mangel en betydelig global trussel, da fiksering av nitrogen fra atmosfæren er ansvarlig for 1% av energiforbruket og 1,4% av CO_2- fotavtrykket på global skala. «Peak phosphorous» teorien beskriver hvordan verden vil gå tom for fosfor ved slutten av dette århundre, som utgjør en alvorlig trussel mot verdens matsikkerhet.

Målet med denne studien var å adressere utfordringene knyttet til håndtering av næringsstoffer i RAS, som utgjør en lokal bekymring, samtidig som nitrogenmangel representerer et globalt problem. Ved å dyrke mikroorganismene som naturlig finnes i RAS vann som biofilm i en bioreaktor, kan dette systemet utnytte næringsstoffene i RAS vannet og samtidig bidra til vannrenseprosessen. I tillegg kan biofilmproduktet høstes og brukes som mulig fôringrediens eller gjødselkomponent på grunn av den verdifulle biokjemiske sammensetningen assosiert med mikroalger. Formålet med denne studien var å bidra til utvikle av et vekstsystem for mikroorganismer i RAS-vann fra Hardingsmolt AS. Viktige faktorer som påvirket utviklingen og dyrkingen av biofilmen ble karakterisert. I tillegg ble den biokjemiske sammensetningen i biofilm produktet, produsert under forskjellige høstfrekvenser, bestemt og sammenlignet med biomassene fra en pilotstudie utført på Hardingsmolt RAS anlegg.

Et sentralt funn var at fotoautotrofe organismer dominerte biofilmkonsortiet, noe som indikerer at lys er en viktig faktor for dyrkingen. Videre økte biomasseutbyttet og produktiviteten betydelig med tilsetning av silikat til RAS-vannet, opprettholdelse av høy næringskonsentrasjon og høsting av biofilmen hver 12. dag. Den biokjemiske profilen til biofilmproduktet under påvirkning av forskjellige høstfrekvenser (4 dager, 8 dager, 12 dager) ble karakterisert. Betingelsen med 12 dagers høstfrekvens hadde en signifikant høyere verdi innenfor total protein (363 mg g^{-1} DW), carbon og nitrogen innhold og sum ikke-essenielle amino syrer (208 mg g^{-1} DW). Når biofilmproduktet fra laboratoriet ble sammenlignet med produktet fra pilotreaktorene ble det ikke funnet signifikante forskjeller. De verdifulle flerumettede fettsyrene: eikosapentaensyre (EPA) og dokosaheksaensyre (DHA) var til stede i alle gruppene, der 12 dagers høstfrekvens hadde et noe høyere, men ikke signifikant, høyere innhold. Også høye nivåer av palmitoleinsyre ble funnet i alle gruppene.

Resultatene fra denne studien demonstrerte en vellykket dyrking av biofilm på mikroorganismer fra RAS vann (Hardingsmolt AS). Biofilm produktet ble anerkjent som en lovende komponent både for behandling av RAS vann og som en potensiell ingrediens i fôrproduksjon.

Table of Contents

List of Figures

List of Tables

List of Abbreviations

AA	Amino acid
AOB	Ammonia oxidizing bacteria
AWW	Aquaculture wastewater
C	Carbon
DW	Dry weight
DHA	Docosahexaenoic acid
EAA	Essential amino acid
EFA	Essential fatty acid
EPS	Extracellular polymeric substances
EPA	Eicosapentaenoic acid
FA	Fatty acid
FAME	Fatty acid methyl ester
GC	Gas chromatography
HGT	Horizontal gene transfer
NEAA	Non-essential amino acid
N	Nitrogen
NH_4^+	Ammonium
NO_2^-	Nitrite
NO_3^-	Nitrate
NOB	Nitrite oxidizing bacteria
NTNU	Norwegian University of Science and Technology
OD	Optical density
P	Phosphorous
PA	Palmitoleic Acid
PUFAs	Polyunsaturated fatty acids
QS	Quorum sensing
RAS	Recirculating Aquaculture Systems
Rpm	Rounds per minute
SE	Standard Error
SGR	Specific growth rate
TAN	Total ammonium nitrogen
TBS	Trondhjem Biological Station
TEP	Transparent exopolymer particles
TL	Total lipid

TP	Total protein
TCP	Total crude protein
4DHF	4 days harvest frequency (condition)
8DHF	8 days harvest frequency (condition)
12DHF	12 days harvest frequency (condition)
+ Si	Addition of silica (condition)
- Si	No addition of silica (condition)

1 Introduction

An increasing demand for fish and seafood combined with a decrease in wild fish harvest, is driving the aquaculture industry at a rapid pace. Aquaculture is now the fastest growing sector in the food industry and provides nearly 50% of the fish for human consumption (Ansari et al., 2021). Due to this intense development, concerns are being raised regarding overexploitation of raw materials used for fish feed production, as well as the environmental pollution associated with aquaculture wastewater (AWW) (Tossavainen et al., 2019a). The high demand for consumption of the modern society cannot be met by the limited resources of nature and therefore calls for new sustainable feedstock alternatives.

Regarding both wastewater remediation and substitutes for fish feed ingredients, the industry is increasingly turning towards microalgae for sustainable solutions. Microalgae have a well-balanced and valuable nutrient profile, rich in protein, lipids, and carbohydrates, in addition to a net biomass productivity higher than any terrestrial plant or animal, thus being an ideal candidate as a feed ingredient (Chauton et al., 2015, Reitan et al., 2021). Because of the high nutrient removal efficiency from e.g., AWW, there has been an increased interest on implementing microalgae as a part of the wastewater treatment processes (Stevčić et al., 2019). Consequently, utilizing microalgae in wastewater treatment has the potential to lower the energy consumption, increase the nutrient removal efficiency while simultaneously producing valuable biomass for sustainable feed production, contributing towards a bio-circular approach.

1.1 Recirculating aquaculture systems

Over the past decades, in line with an increased pressure on freshwater resources, there has been an increase in the use of recirculating aquaculture systems (RAS) (Ahmed and Turchini, 2021). RAS is an alternative production method to the traditional flow through water system often used in land-based aquaculture farming (Ahmed and Turchini, 2021). In RAS, the wastewater is processed through a multistep water treatment process, allowing the water to be recycled back to the fish tanks and therefore reducing the water consumption and allowing for temperature control (Wold et al., 2014, Ahmed and Turchini, 2021). This makes RAS a sustainable and highly efficient way of producing aquatic species such as Atlantic salmon (*Salmo salar*) (Ahmed and Turchini, 2021). A key aspect of RAS is the biofilter, in which a unique microbial community mediates the water treatment process (Almeida et al., 2021).

The specific design of RAS differs depending on the supplier; however, the system design can be explained in general terms and are schematically presented in Figure 1. Feed is metabolized by the fish to biomass, feces, urea, CO_2 and total ammonium nitrogen (TAN), which at high concentrations are toxic to the fish (Tom et al., 2021). Thus, as the fish's

metabolism affects the water quality, along with unneatened feed particles, the water needs continuously cleansing through both mechanical and biological filtration (Badiola et al., 2018). Particulate material, such as feed and feces, are removed by the use of mechanical filters where drum- or belt filters are the most common (Fjellheim, 2017). After the mechanical filtration, the water is treated in a biofilter that facilitates the nitrification process, where ammonia (NH_3) is first converted to nitrite (NO_2^-) and subsequently nitrate (NH_3^-) (Tom et al., 2021). This is done by nitrifying bacteria that are normally organized in a biofilm attached to a surface (Tom et al., 2021, Rojas-Tirado et al., 2019). The nitrifying process is presented below in Equation 1 and 2 (Chen et al., 2006).

$$NH_4^+ + 1.5O_2 \rightarrow NO_2^- + H_2O + H^+ (Nitrosomonas\ sp.) \quad 1$$

$$NO_2^- + 0.5O_2 \rightarrow NO_3^- (Nitrobacter\ sp.) \quad 2$$

In the first step of the nitrifying process (Equation 1), NH_4^+ is oxidized to NO_2^- by ammonia oxidizing bacteria (AOB), here *Nitrosomonas* is given as example. In the second part of the nitrifying process (Equation 2), NO_2^- is oxidized to NO_3^- by nitrite oxidizing bacteria (NOB) such as e.g., *Nitrobacter*. Compared to NH_4^+ and NO_2^-, NO_3^- is less toxic to the fish, however, when present in very high concentrations NO_3^- can also have negative physiological effects on the fish (Davidson et al., 2017).

Today, two main solutions targeting the challenge of NO_3^- accumulation are available: denitrification and dilution with a higher water exchange rate (Preena et al., 2021). Increasing the water exchange rate is naturally an unpopular solution due to the desire of minimizing the water usage for environmental reasons. The denitrification process is the reduction of oxidized forms of nitrogen (N), such as NO_3^- to nitrogen gas (N_2), utilizing organic matter (Szatkowska and Paulsrud, 2014). However, as organic matter in RAS is hard to degrade, an organic matter source e.g., methanol, is typically added to increase efficiency, making denitrification a costly process (Szatkowska and Paulsrud, 2014, van Rijn and Barak, 1998). Nevertheless, binding N from the atmosphere is responsible for 1% of the energy consumption and 1.4% of the CO_2 footprint on a global scale (Gür, 2022). The high N levels pose a local challenge in RAS, while N deficiency represents a significant global issue. Therefore, by utilizing N from RAS as a fertilizer or feed directly, it will lower a pressure of producing fertilizer or feed, thus lower the energy and carbon (C) footprint.

To utilize the N in RAS, researchers have been facing towards microalgae. Microalgae cultivation as an integrated system in RAS is not a much-trodden territory, however, there has been an increased interest over the past years (Villar-Navarro et al., 2021). Microalgae can utilize dissolved nutrients in RAS water, such as NO_3^-, to generate algal biomass, while simultaneously optimizing the water treatment process by reducing the dissolved N in the RAS water (Villar-Navarro et al., 2021). Furthermore, the algal biomass is associated with a valuable biochemical composition, rich in protein and lipids, which could be ideal as e.g., feed substitute, enforcing the principle of circular bio-economy (Tossavainen et al., 2019b).

The implementation of microalgae in future RAS facilities holds great potential for producing healthy fish compatible with environmental sustainability by lowering the energy consumption and CO_2 footprint. Simultaneously, possible feedstock ingredient can be obtained as a biproduct.

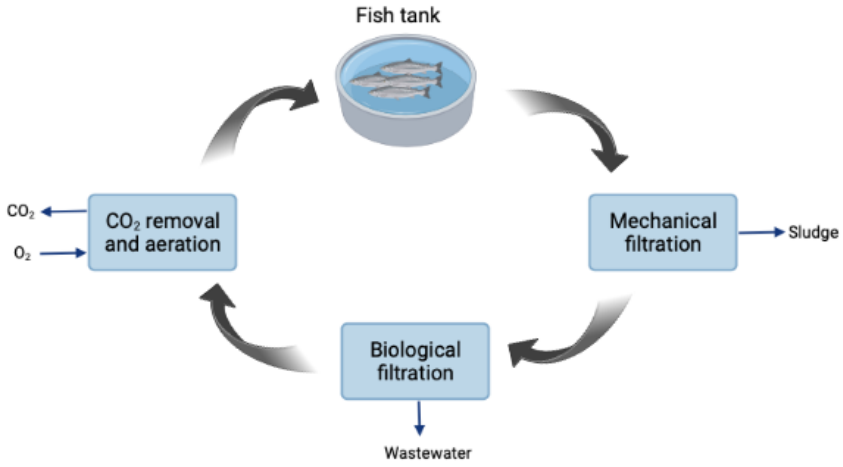

Figure 1: A simple schematic overview of the main components in the wastewater treatment process in recirculating aquaculture system (RAS). The flow of the water is indicated by arrows, flowing from the fish tanks through mechanical filtration where particulate matter is removed, biological filtration where wastewater is removed, before CO_2 is removed by the water and O_2 is added. Purified and O_2-enriched water is then returned to the fish tanks. Illustration made using Biorender.

1.2 Microalgae

Microalgae are eukaryotic, unicellular and photosynthetic microorganisms (Ruane et al., 2010). Like plants, microalgae are capable of photosynthesis thanks to their specialized organelle called chloroplast, where they convert light, inorganic nutrients, H_2O and CO_2 into sugars (Ruane et al., 2010). They are important primary producers in a broad range of aquatic environments, including oceans, ponds, rivers, lakes and even wastewaters, and can adapt to various temperatures, pH values, salinities and light intensities (Khan et al., 2018). Reflecting on the diversity in biochemistry, ultrastructure, physiology and genetics, microalgae are truly remarkable organisms (Andersen, 2013). The diatom cell wall for instance, which is the main characteristic feature of the diatom, provides a picture on how different some of the microalgae species are from each other. Diatoms are brown algae belonging to the class of Bacillariophyceae (Round et al., 1990). The diatom cell wall is made up of two silicified, unequal halves, called epivalve and hypovalve (Round et al., 1990). These parts fits together like a lid on a box, and siliceous bands holds the structure together (Round et al., 1990). However, looking at the cell wall composition in other microalgal species, cellulose or complex polysaccharides are often seen to dominate the structure (Alhattab et al., 2019). Although the diversity of microalgae species is substantial, making generalizations difficult, diversity is also what has drawn researchers into investigating the many aspects of microalgae (Singh and Saxena, 2015).

Extensive research has unlocked a lot of hidden potential of microalgae, and one noteworthy characteristic is their ability to utilize inorganic and organic C, N and phosphorus (P) along with other nutrients in e.g., wastewater effluents, to produce biomass (Wang et al., 2022). They have also emerged as excellent candidates for CO_2

capture, as microalgae, when compared to some terrestrial plants, can be up to ten times more efficient in fixing CO_2 (Russell et al., 2021, Chauton et al., 2015). One aspect that seem to be of interest is the valuable biochemical profile and the array of bio-active compounds that can be extracted from microalgal biomass (Wang et al., 2019). In general, the microalgal biomass contains high amounts of valuable products such as e.g., carotenoids (pigments), protein, polyunsaturated fatty acids (PUFAs) and lipids (Russell et al., 2021, Gauthier et al., 2020). However, this profiling is highly dependent of the species that is being considered as it can vary drastically. Microalgal biomass is currently being utilized in feed and biofuel production, in pharmaceuticals and medical applications, and in the food production industry (Russell et al., 2021, Devi et al., 2022). Even though microalgae cultivation and production have faced some bottlenecks, especially regarding costs and challenging harvesting procedures, the valuable aspects of microalgae seem to advance both research and the industry (Wang et al., 2022). Products deriving from microalgae or that utilizes microalgae biotechnology are considered more sustainable alternatives, thus provide environmental benefits (Olaizola and Grewe, 2019).

1.3 Cultivation of microalgae and its optimal influencing factors

Microalgae cultivation has been extensively studied, resulting in the development of numerous systems (Tang et al., 2012, Rana and Prajapati, 2022, Zou et al., 2021, Chiaramonti et al., 2013). These systems normally fall into two categories: as suspended cultures where the microalgae cells flow freely in the culturing medium, or as attached cultures where microalgal cells grow as a biofilm attached to a surface (Mantzorou and Ververidis, 2019, Dalirian et al., 2021, Rosli et al., 2020). Suspended cell culturing systems is the more conventional system often used for wastewater treatment (Pires et al., 2013). However, this traditional way of culturing microalgae suffers from a major drawback concerning the biomass harvesting, which is costly, energy intensive and time consuming (Zhuang et al., 2018). Meanwhile, attached cultures can grow quite densely and can easily be scraped off mechanically, resulting in an easy and cost effective harvest method (Zhuang et al., 2018). Research by Zhuang et al. (2018) highlighted the benefits of attached systems, including higher productivity and enhanced water treatment capabilities (Zhuang et al., 2018). Still, attached cultivation methods present challenges due to a relatively short research period, entailing certain knowledge gaps on e.g., microalgal attachment mechanisms and factors influencing attached growth (Wang et al., 2018). Nevertheless, attached cultivation of microalgal biomass holds great potential in addressing various global challenges affecting the world today.

Microalgae need light, CO_2 and nutrients to grow, however other factors are affecting the growth, especially in the aspect of cultivation (Olaizola and Grewe, 2019). Amongst these factors are pH, temperature, light intensity, and substrate modification (Cheah and Chan, 2021). In addition, the specifics of the cultivation system, may also influence the response on microalgae growth and biochemical composition, even when all necessary conditions (nutrients, light, etc.) are met (Zhuang et al., 2018).

1.3.1 Nutrient requirements

Microalgae require a distinct supply of macro-, and micronutrients for optimal growth (Estevam et al., 2022). Macronutrients include C, N and P, and silica (SiO_2) in the case of diatoms (Estevam et al., 2022). Vitamins and trace metals are micronutrients and are needed in smaller amounts (Estevam et al., 2022). Each species have different nutritional requirements and require specific concentrations of each nutrient (Estevam et al., 2022). Furthermore, as microalgae grow, their nutritional requirements changes throughout the lifespan of the growth phase (Mantzorou and Ververidis, 2019). For instance, during biofilm formation, nutrient availability is crucial (Katarzyna et al., 2015). However, due to ineffective cell settling and correction during the beginning of the growth phase, nutrient uptake is typically decreasing a bit (Mantzorou and Ververidis, 2019). When the biofilm matures, the nutrient uptake increases and the growth will go into a steady state (Mantzorou and Ververidis, 2019). Finally, the nutrient uptake decreases when the biofilm enters the death phase (Mantzorou and Ververidis, 2019).

By manipulating the nutrient concentration, especially P and N which are crucial for growth, the metabolism of the microalgae can shift to induce biosynthesis of certain metabolisms (Estevam et al., 2022). One component that has been intensively studied regarding nutritional stress for increased biosynthesis, are lipids. By introducing nutritional stress to microalgae by, for example inducing a N limitation, lipid content can significantly increase (Chen et al., 2017). This is explained by the fact that during a nutrient deprivation, protein synthesis is limited. However photosynthesis is not necessarily limited as long as sufficient light energy and C is available, thus photosynthesis products accumulate (Li et al., 2020). There are examples of microalgal species who have doubled their lipid yield (in dry cell weight) during N limitation, *Nannochloropsis sp.* being an example (Chen et al., 2017). However, as N is also crucial for growth of the microalgal cell, N limitation and nutrient limitation in general, will be limiting for the cell growth and development in the long run (Chen et al., 2017). Studies have also been made on other high-value products such as proteins, pigments and carbohydrates and their possible effects from inducing stress, however, these studies are not as abundant as the ones on lipids (Chen et al., 2017).

1.3.2 Light

As light is the main energy source that drives photosynthesis, microalgae are strongly dependent on light availability for growth and development (Mantzorou and Ververidis, 2019). Aside from optimal growth, light is also important for the actual adhesion of algal cells to surfaces, in the aspect of biofilm formation (Mantzorou and Ververidis, 2019). Nevertheless, growth can be inhibited as a result of too much light (photoinhibition), in which the excessive light absorption can lead to the formation of free radicals (singlet oxygen) causing photo damage to the cell (Lehmuskero et al., 2018). Taking microalgal biofilm as an example, photoinhibition would typically occur at the surface or upper layers of the biofilm (Mantzorou and Ververidis, 2019). However, growth can also be limited by too little light (photo limitation), where the cell consumes the high C compounds faster than what it can produce through photosynthesis, thus lowering the growth rate

(Lehmuskero et al., 2018). Photo limitation normally occurs in the deeper layers of the biofilm (Kesaano and Sims, 2014).

The optimal light intensity varies with the microbial community present and its surrounding environment (Kesaano and Sims, 2014). The distribution of light in microalgae biofilm cultivation, have been extensively studied as light is generally found to be the main factor to limit growth in a cultivation context (Ma et al., 2023). As light passes through the biofilm, parts of the light is absorbed by the pigments inside the cells, where the light energy is converted to biochemical energy through the process of photosynthesis, and thereafter to be used for growth, metabolic processes and cell respiration (Lehmuskero et al., 2018). The other part is scattered by the cell, decreasing the intensity of the light as its passing through the deeper parts of the film (Ma et al., 2023). However, managing to provide sufficient light energy to all layers of the biofilm without reaching neither photoinhibition nor photo limitation is challenging. Ma et. al. recently found that providing light from both sides of the biofilm greatly improved the light distribution (Ma et al., 2023).

Another interesting topic is how the microalgal biofilms adapt to manage various light intensity in its environment (Wang et al., 2021). Wang and colleagues presented a study that was conducted on *Chlorella sp*. biofilms, where different variables were investigated in regard to a series of light intensities (20, 50, 100, 200, and 400 μmol m^{-2} s^{-1}) (Wang et al., 2021). Their study revealed that high light intensities promoted a more dense biofilm as a mechanism of protecting its cells from photo damage, whereas under low light intensities a more porous microstructure formed (Wang et al., 2021). Light spectra have also proven to affect several properties of the microalgal biofilm. Yuan et. al. found that blue and red light were more efficient than white light regarding cell growth, blue light gave the highest photosynthetic and photoprotective capabilities, and higher lipid yield. Whereas, red light gave a higher carbohydrate accumulation (Yuan et al., 2020). These different light-related factors must all be considered to achieve the ideal light intensity for the specific cultivation system, as they all have a big impact on the growth, development, biochemical composition, and robustness of the biofilm.

1.3.3 pH and CO_2

The pH is an important environmental factor for microalgae cultivation. pH determines both the CO_2 availability and solubility, and is strictly related to the microalgal metabolism (Qiu et al., 2017). The cell cycle regulation, protein folding, membrane transport and enzymatic activity are some examples of crucial processes and activities that are contingent on the pH (Zuccaro et al., 2020). One example of the high influence of pH is the enzyme ribulose bisphosphate carboxylase/oxygenase (RuBisCO) which catalyzes the entry of CO_2 molecules into the Cavin- Benson cycle and is therefore dictating the photosynthetic rate, and is highly dependent on pH (Azizi et al., 2020). Consequently, pH is directly linked to the enzymes and processes driving photosynthesis, thus the biomass growth of microalgae and other photosynthetic organisms for that matter.

Furthermore, pH also determines the solubility and availability of CO_2. When CO_2 dissolves in water, it can exist in different forms of inorganic C species depending on the pH (Meier et al., 2022). The different C species include carbon dioxide (CO_2), bicarbonate (HCO_3^-), carbonic acid (H_2CO_3) or carbonate (CO_3^-), although, CO_2 is quickly converted to H_2CO_3 and these two C species will therefore be considered the same (Meier et al., 2022). Figure 2 presents the relative concentrations of carbonic acid (H_2CO_3), bicarbonate (HCO_3^-) and carbonate (CO_3^-) under different pH concentrations (Walter K. Dodds, 2010).

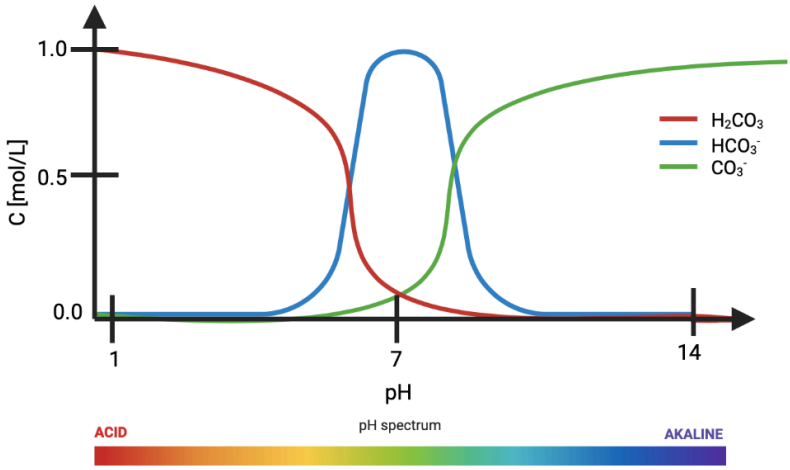

Figure 2: The relative concentrations of three inorganic C species as a function of pH. Schematic is modified from (Walter K. Dodds, 2010) using Biorender.

The conversions of these inorganic C species are called the bicarbonate equilibrium and is important for the understanding of how CO_2 is available for photosynthesis at different pH concentrations (Walter K. Dodds, 2010). The bicarbonate equilibrium equation is presented in Equation 3.

$$CO_2 + H_2O \leftrightarrow H_2CO_3 \leftrightarrow H^+ + HCO_3^- \quad (3)$$

Microalgae can utilize CO_2 or HCO_3^- as C source for photosynthesis, and are therefore dependent on the specific pH levels in which these two C sources are available (Meier et al., 2022). Moreover, different microalgae species can have different pH preferences, although most microalgae have optimal growth at a pH between 7 and 9 (Meier et al., 2022). In the aspect of industrial cultivation, knowing the optimal pH of the chosen microalgae is therefore crucial to ensure maximum growth.

1.4 Microalgal biofilm

In nature, it is extremely rare to find microorganisms living in isolated pure cultures (Flemming and Wingender, 2010). They commonly form aggregates and communities crossing phylum, class, genera and species (Flemming and Wingender, 2010). A biofilm is a complex structure in which a consortium of microorganisms, embedded in extracellular polymeric substances (EPS), are living in an interface between a solid surface or support media, and a liquid phase (Fanesi et al., 2019, Schnurr and Allen, 2015). The EPS, which often constitutes as much as 90% of the biofilm, has various important functions, such as facilitating intense cell-cell communication, serving as a nutrient source, and it provides the embedded microorganisms protection against its surrounding environment (Flemming and Wingender, 2010, Cheah and Chan, 2021).

Biofilms can arise in a wide range of environments, and the composition of the biofilm and the EPS production will be dictated by the environmental niche present (temperature, pH, light and nutrient availability) (Cheah and Chan, 2021). An in- depth description of the biofilm formation process is presented in Appendix G. Biofilms can consist of a broad spectrum of organisms, where bacteria, algae, fungi, or other microorganisms form biofilm together (Luo et al., 2022). However biofilms can also consists purely of e.g., bacterial strains or it can be heavily dominated by one species and even form monocultures (Luo et al., 2022). The term mixed microalgal biofilm refers to a biofilm dominated by microalgae, however, other microorganisms are generally also present, bacteria being an almost obvious participant (Berner et al., 2015). In nature, there are several examples of bacteria and algae forming complex microbial communities where specific activities executed in the community are dependent on the presence of both participants (Yao et al., 2019). Several examples of algae-bacteria interactions in a biofilm have been described, where nutrient exchange, signal transduction and gene transfer are some examples (Kouzuma and Watanabe, 2015). A biofilm is therefore a highly complex system, where several species of microorganisms live in symbiosis and conduct specific activities.

In society, microbial biofilms have been both the cause and the cure to numerous ancient and emerging challenges, including water pollution, fouling and antimicrobial tolerance (Seviour et al., 2019). Still, many of the basic questions regarding biofilm establishment and functions remain unanswered, despite being a hot topic among researchers (Seviour et al., 2019). Up to now, scientists have been focusing their efforts on development and cultivation of microbial biofilm for industrial purposes (Cheah and Chan, 2021). This have resulted in numerous applications for microbial biofilm such as wastewater treatment and as a feedstock- ingredient. Research has also provided valuable knowledge on the benefits of cultivating biofilms compared to other microbial systems, such as planktonic cultures, where cells float freely in cultivation media (Kilbane, 2022). In wastewater remediation, using biofilm will decrease the cost of harvesting compared with the energy demanding harvesting and dewatering processes of a planktonic culture, which often include energy demanding methods such as centrifugation (Hu et al., 2021). Also, in some planktonic cultures, chemicals such as aluminum ions and polyacrylamide are added for flocculation, which may have harmful effects (Hu et al., 2021). Such chemicals are not needed for biofilm cultivation and can therefore ensure biomass safety. Biofilm communities are also known to be more robust and can tolerate small changes in the environmental conditions that may occur in the wastewater treatment process (Kilbane, 2022). As the field of using

biofilms for wastewater treatment is highly popular due to interesting findings and success on industrial applications, as well as being advantageous over other cultivation methods, research is constantly driving the cultivation technology development.

1.4.1 Microalgal biofilm composition

The biochemical composition of microalgae biofilm can vary greatly depending on the species composition. However, there are certain components that stand out in being similar for all biofilms; the biofilm matrix, or more specifically the EPS, being an important common denominator (Flemming and Wingender, 2010). The EPS is actively produced by the microorganisms making up the biofilm and constitutes as much as 90% of the organic matter (Cheah and Chan, 2021). Looking at the three- dimensional architecture of the biofilm EPS; water, polysaccharides, proteins, lipids, and nucleic acids are the main components as visualized in Figure 3 (Cheah and Chan, 2021, Sutherland, 2001). These macromolecules interacts with each other to maintain a stable matrix (Cheah and Chan, 2021). Polysaccharides play an important role in the matrix by enhancing biofilm-to-substrate adhesion by providing elasticity and shape (Cheah and Chan, 2021). Proteins function in cell-cell communication, enhance the tolerance to the microenvironment during water deficiency, and function in digestion of exogenous macromolecules for nutrient accession (Cheah and Chan, 2021). Lipids serve as bio- surfactant and bio-emulsifiers (Cheah and Chan, 2021). The biochemical composition of the microalgal biofilm has been studied extensively, as it has proved to be highly valuable for many industries. Aquaculture in particular have found microalgae interesting due to the respective high protein and lipid content that are associated with certain microalgal strains (Shah et al., 2018).

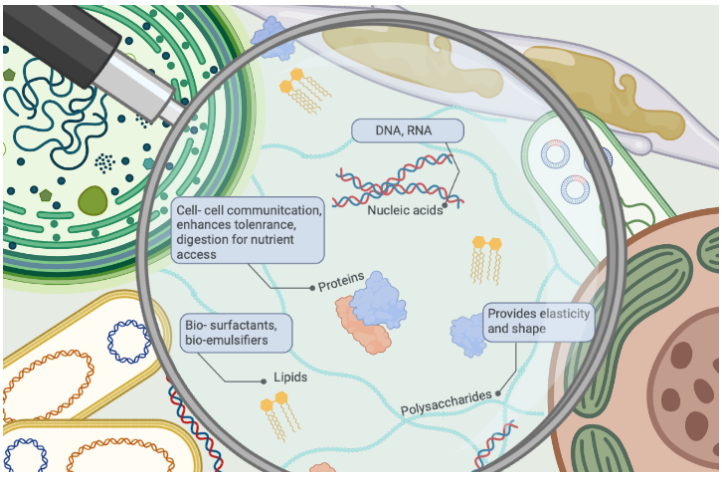

Figure 3: A visual presentation of the main components of the microalgal biofilm and extracellular polymeric substances (EPS), and their functions. Modified from (Seviour et al., 2019) using Biorender.

1.5 Microalgae as an aquaculture feed- ingredient

In recent years, microalgae have been considered as a possible feed substitute for the aquaculture industry. The rapid growth of the aquaculture sector calls for new, sustainable feed alternatives, as fish meal, fish oil and soybean have become unsustainable feed options (Ahmad et al., 2022, Chauton et al., 2015). Despite being good protein and lipid sources, fish meal and fish oil are putting pressure on wild fish resources and can lead to an imbalance in the marine ecosystems (Malcorps et al., 2019, Chauton et al., 2015). Soy is labeled unsustainable for several reasons, some of which being deforestation and high water usage, in addition to a high use of agrochemicals (Jia et al., 2020). Microalgae in particular have been suggested as an alternative feed candidate for numerous reasons, two examples are the high net biomass productivity and valuable nutrient composition (Chauton et al., 2015). By producing microalgae on-site, the transportation aspect will be highly limited compared to other options, such as soy, which must be transported over great distances (da Silva et al., 2010).

Feed used in aquaculture must contain certain components that cover the fish's essential need for maximal growth, ability to defeat disease and obtain high flesh nutritional value (Prabu et al., 2017). To achieve this, a diet with the right content of amino acids (AA), lipids, minerals and vitamins is needed (Prabu et al., 2017). The valuable nutrient profile of microalgae has great potential as a nutritional supplement. It provides protein important for individual growth, along with essential amino acids (EAA) which the fish cannot produce itself and must therefore get from its food source (Nagarajan et al., 2021). Microalgae are also rich in valuable lipids containing PUFAs, including eicosapentaenoic acid (EPA) and docosahexaenoic acid (DHA) (Ahmad et al., 2022). EPA and DHA are essential fatty acids (EFA) that are highly important in cell membrane functionality and viscosity and have shown to have anti-inflammatory properties in animals and humans (Swanson et al., 2012). This enhances proper neuronal, retinal and immune function, fetal development, thus healthy aging (Swanson et al., 2012). EPA and DHA have also been linked to prevention of diseases such as several cardiovascular diseases and Alzheimer's disease (Swanson et al., 2012). Most animal species cannot synthesize EPA and DHA but rely on the assimilation of these lipids from their food source. Moreover, these fatty acids (FA) are quite difficult to synthesize in the lab, making microalgae a highly valuable feed ingredient.

Nevertheless, the beneficial characteristics of microalgae do not end here. As microalgae are photosynthetic species, they naturally contain a substantial amount of piments (Nagarajan et al., 2021). The aquaculture industry have a high usage of pigments, especially astaxanthin which is used as a colorant for crab, shrimp and salmonoid fish (Nagarajan et al., 2021). Aside from their appealing color, pigments have several benefits. Pigments are antioxidants, vitamin precursors, they have anti- inflammatory properties and work as neuroprotectants (Ahmad et al., 2022). Unlike some of today's synthetic pigments, which have been questioned regarding their possible negative health effects, the pigments deriving from microalgae are a natural and health- promoting alternative (Ahmad et al., 2022). Villar-Navarro and colleagues showed that an addition of 20% microalgae (*Tetraselmis chui*) in the feed formulation did not negatively affect the fish growth or the fillet quality of *Solea senegalensis*, but contributed to an increased immunological activity (Villar-Navarro et al., 2022).

In addition to the ideal biochemical content, using microalgae offer several advantageous characteristics. Unlike terrestrial crops or animals, microalgae can be cultivated without the need of soil or land. Microalgae can grow using wastewater from various sources, including RAS water that holds substantial amounts of P and N (Villar-Navarro et al., 2022). Through the implementation of on-site bioreactors, microalgae can utilize nutrients in RAS water to generate biomass for possible feedstock supplements, while simultaneously partitioning in the water treatment process by removing N and P. This approach presents promising solutions to address both the local challenge of nutrient accumulation in RAS and the global N and P deficiency. Figure 4 summarizes the potential solutions implementing microalgae in RAS. The role of microalgae in wastewater remediation has already been successfully employed in various industrial wastewaters and domestic sewage, such as in RAS or municipal water treatment plants, to meet the rising challenges of both water scarcity and nutrient accumulation (Seviour et al., 2019). Consequently, microalgae can offer financial, environmental, and nutritional advantages over alternatives like soybean, fish meal, and oil that are no longer regarded as sustainable, thereby strengthening the concept of circular bio-economy.

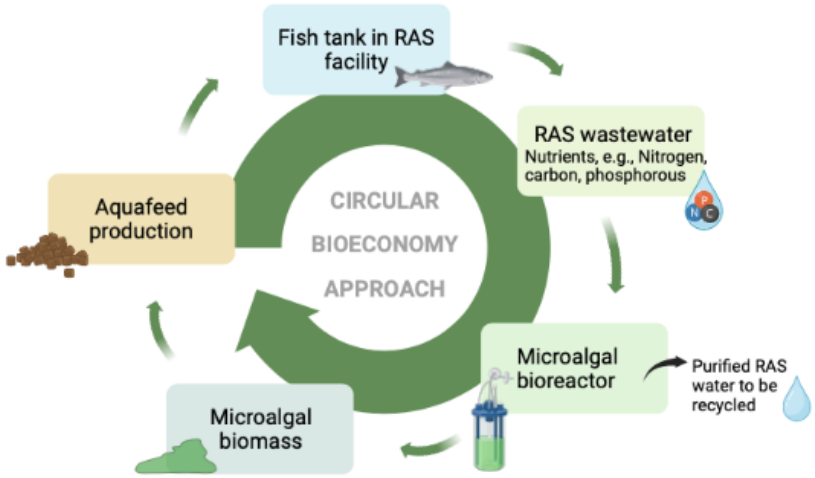

Figure 4: The principle of circular bioeconomy applied to using microalgae for both wastewater remediation and as a feed ingredient. Nutrients in wastewater from RAS utilized in microalgal bioreactors as a part of the water treatment process in addition to harvesting the algal biomass for aquafeed production. The illustration is modified from (Bongiorno et al., 2022) using Biorender.

1.6 Aim of study

This study aimed to develop a growth system for cultivating mixed community of microorganisms present in the RAS water from Hardingsmolt AS, and to characterize the biochemical composition of the biomass produced. To do this, crucial influencing factors for biofilm development and cultivation had to be determined. Additionally, the biochemical composition of the biofilm product, under different harvest frequencies, was also determined. Finally, a pilot study on-site at Hardingsmolt AS was performed to compare the biochemical profiles of that biofilm and what were obtain in the lab at different harvest frequencies.

To identify influencing factors for biofilm development and for the biochemical characterization of the biofilm product, four subgoals were defined:

I. *The effect of light intensity* on the growth of the microbial community cultivated on RAS water from Hardingsmolt (Experiment I).

II. *The effect of silica addition* to the RAS water from Hardingsmolt on growth and biomass productivity of the microbial community (Experiment II).

III. *The effect of nutrient concentration* of the Hardingsmolt RAS water on the growth and biomass development (Experiment III).

IV. *The effect of harvest frequency* on the biofilm cultivated on RAS water from Hardingsmolt on biomass productivity, and its biochemical composition (Experiment IV).

1.6.1 Hardingsmolt pilot study

Two pilot reactors were placed at Hardingsmolt RAS facility to test two reactor designs (The specific designs are confidential) and their ability to cultivate biofilm from the microorganisms present in the RAS water. Samples were collected to investigate the biochemical composition of the biofilm and the results were compared with the lab experiments.

1.7 Collaboration

All cultivation experiments were carried out in collaboration with another master student, Johan Edvard Iversen, who focused on the species composition of the microbial community of the biofilm and conducted a genetic analysis (DNA sequencing; Illumina and Nanopore).

2 Materials and methods

2.1 Collection of RAS water

RAS water was delivered from Hardingsmolt AS, a RAS facility located in Tørvikbygd, Hardanger. Hardingsmolt AS is commercially farming post smolt of Atlantic Salmon (*Salmo salar*). The temperature of the facility was kept at 13°C and the water had a salinity of 15 ppt. The RAS water used in this study was collected after the mechanical particle filtration step (drum filter) in 100L cans and shipped to the lab (NTNU Sealab, Brattøra). Aside from the testing conditions (+/- silica (exp II) and nutrient concentration (exp III)), no modifications of the RAS water were made. Water was collected at different time points and therefore the water characteristics of each specific experiment conducted (start water of each experiment) is described. Characteristics of the RAS start water is presented in the result section in Table 3.

2.2 Sampling, acronyms and analyses

An overview of the four experiments and pilot study, with the respective testing variables and conducted analyses, as well as the acronyms used for the respective conditions are presented in Table 1. The possible analyses conducted were respectively, biomass (growth measurements) (g m^{-2}), specific growth rate (SGR) (day^{-1}) and productivity (g m^{-2} day^{-1}), and several biochemical analyses. The specifics of the biochemical analyses are presented in section 2.4.3.

Table 1: The testing variables and conducted analyses of each experiment in this study, in addition to the acronyms used. The completion of an analysis is indicated with "X".

Experiment	**Testing variable(s)**	**Acronyms**	**Analyses**		
			Biomass	**SGR* and productivity**	**Biochemical analyses**
Experiment I-*effect of light intensity*	High light, medium light, no light				
Experiment II-*effect of silica addition*	Addition of silica, no addition of silica	+Si, -Si	X	X	
Experiment III-*effect of nutrient concentration*	High nutrient concentration, low nutrient concentration		X	X	
Experiment IV-*effect of harvest frequency*	Harvest frequencies of 4 days, 8 days, and 12 days	4DHF, 8DHF, 12DHF	X	X	X
Pilot project at Hardingsmolt	Horizontal growth plates, vertical growth plates		X	X	X

*SGR = specific growth rate

2.3 Experimental setup, procedure and sample collection

2.3.1 Experiment I- Effect of Light intensity

The experimental setup consisted of 12 cell cultivation flasks (areal 75 cm^2, volume 850mL) sat vertically (3 treatments with 4 replicates) with the light source coming from behind, setup is visualized in Figure 5. Three different light intensities, high light: ~240 µE m^{-2} s^{-1}, medium light: ~160 µE m^{-2} s^{-1}, and no light: <20 µE m^{-2} s^{-1}, respectively, were run with four replica each. Light was measured using a light meter (WALZ, ULM-500) and illumination was kept constant (light on for 24 hours). To ensure water movement and aeration, each flask was equipped with an aeration tube (compressed atmospheric air, approx. 3 bubbles pr. sec), where the airflow was filtrated through a 0.22µm hydrophobic filter. All flasks had a pipette with a syringe attached for sampling. To ensure an uncontaminated environment in the cell cultivation flasks, the cap was replaced with cotton balls. The experiment was carried out in a temperature-controlled room, at 13°C (The temperature of the RAS facility). All equipment was sterilized by either autoclavation or acid bath (HCL [32%] and dH_2O).

All flasks were inoculated with 85 mL pure RAS water (RAS water directly from the RAS facility) added to the remaining 765 mL of autoclaved RAS water, giving a 1:10 ratio.

The experiment lasted for 17 days. Growth was measured spectrophotometrically (OD_{460nm}) using a UviLine 9100. Sampling measurements were conducted daily by taking out 3 mL using the attached syringe (the first 1.5 mL was discarded). First, the pH was measured using a pH meter (PHM210) before the sample was transferred to a cuvette and measured in the spectrophotometer. The results could not be used, as the growth turned out to be of benthic form.

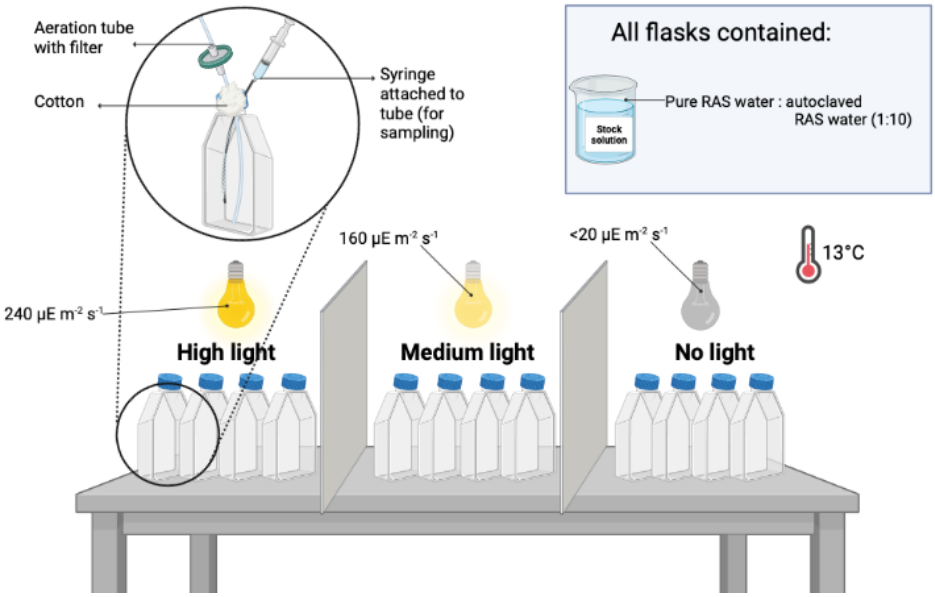

Figure 5: A schematic visualization of the setup of experiment I- effect of light intensity. Illustration made using Biorender.

2.3.2 Experiment II- Effect of silica addition

60 small cell cultivation flasks (areal 25 cm^2, volume 19 mL) were placed horizontally, with constant light coming from above at an intensity of 203-333 µE m^{-2} s^{-1} (light was kept constant). There were two conditions, addition of silica and no addition of silica (RAS water only), respectively. There were 30 replicates pr. condition, and the experimental setup is described in Figure 6. Temperature was kept constant at 13°C. All equipment used was either autoclaved or acid bathed (HCL [32%] and dH2O).

A stock solution was made in a 1:10 ratio. 10% was an inoculum collected from experiment I and the remaining 90% consisted of autoclaved RAS water. Additionally, for the condition with addition of silica, silica was added to the stock solution (Na_2SiO_3-5(H_2O)) with a concentration of 1 µL mL^{-1}. The respective stock solution was distributed to all flasks of the respective condition, with silica addition or without silica addition (19 mL pr. flask).

The experiment lasted for 15 days. Microbial growth was measured daily using an inverse microscope (Nikon eclipse TE2000-S) with a 10x magnification. Pictures were taken at 11 different coordinates on the flasks (the same coordinated were repeated for all flasks). The specific coordinates are presented in Appendix A, Figure A.1. By using ImageJ, the pictures were analyzed by measuring the average %area that was occupied by particles on the surface of the cell cultivation flask.

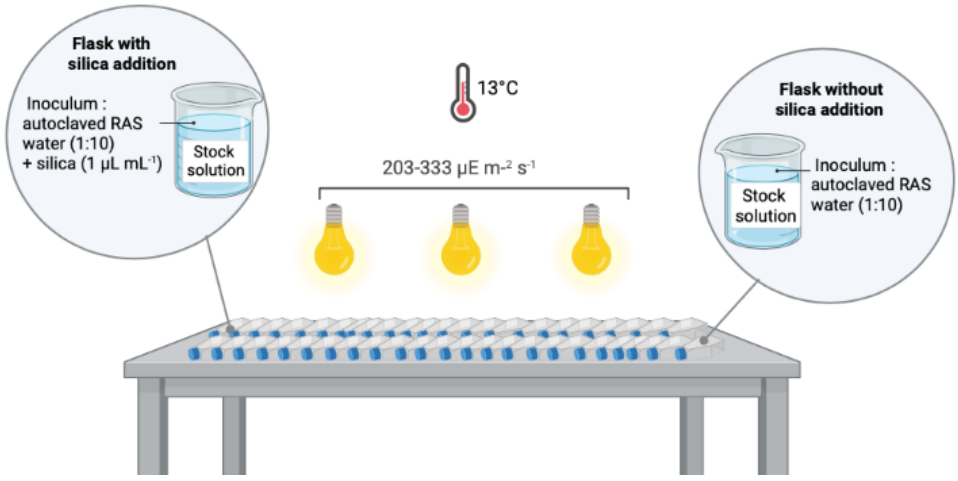

Figure 6: A schematic overview of the setup of experiment II- effect of silica addition. Illustration made using Biorender.

2.3.3 Experiment III- Effect of nutrient concentration in the water

The experimental setup consisted of 60 small cell cultivation flasks (areal 25 cm^2, volume 19 mL) laying horizontally, with constant light coming from above at an intensity of 203-333 µE m^{-2} s^{-1}, and constant temperature of 13°C. Two conditions were investigated: high nutrient (N concentration: 56 mg^{-1} L) and low nutrient (N concentration: 5.6 mg^{-1} L) content. 30 biological replicates were tested for each condition. The setup is visualized in Figure 7. All equipment used was either autoclaved or acid bathed (HCL [32%] and dH2O).

No inoculum was used in this experiment. A stock solution was made with autoclaved RAS water and non-autoclaved RAS water in a 1:10 ratio. For the low nutrient condition, this stock solution was diluted by 10 to reach the low N concentration of 5.6 mg^{-1} L. A nutrient poor water (water collected when fish was on starvation), also coming from Hardingsmolt, was used for the dilution. The respective stock solution was distributed to each flask in the respective condition (19 mL pr. flask). N concentration (NO_3^--N) in the water measured at Hardingsmolt facility on the day of collection was used when calculating the stock solution to ensure right N concentrations, and are presented in Appendix B, Table B.1.

To measure the microbial growth, an inverse microscope (Nikon eclipse TE2000-S) with magnification 20x was used. Pictures were taken as described above (Appendix A, Figure A.1). ImageJ was used to analyze the pictures to find average %area to get a measurement on the growth of the microbial community.

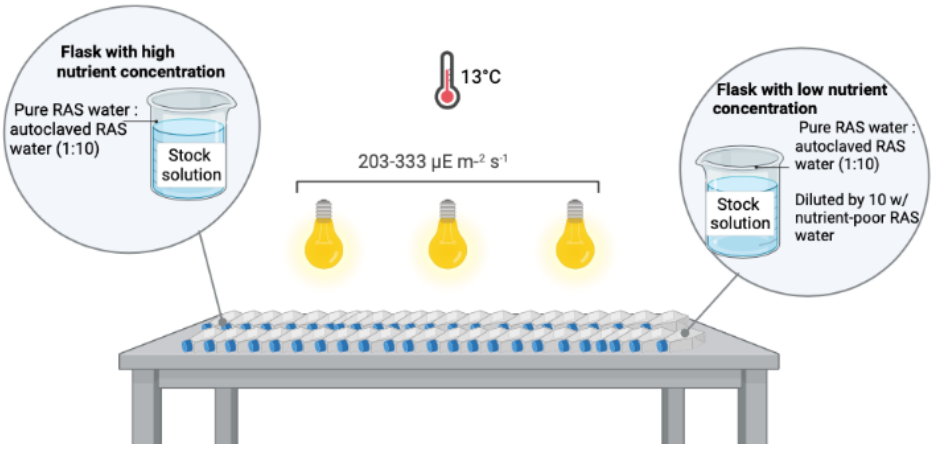

Figure 7: A visual presentation of the setup of experiment III. Schematic made using Biorender.

2.3.4 Experiment IV- Effect of harvest frequency

The experimental setup of experiment IV consisted of 12 separate reactors (0.34m x 0.25m x 0.16m), containing a growth plate (0.26m x 0.19m x 0.005m) made of polyethylene (PE), covered in cotton fabric. The reactors were incubated and acclimated with RAS water in a batch culture for 8 days, whereafter a flow through system was initiated. The experimental period lasted for 36 days. RAS water was pumped from a 50L tank (covered and keep in the dark) and into the reactor by a peristatic pump. The water level was kept constant at 1.25L by a drainage tube that would drain the overflow. The flow rate was kept constant at 0.10L h^{-1} or 1.5L day^{-1}. The 50L tanks with RAS water was refilled according to the water usage. The experimental setup is visualized in Figure 8. Light coming from above was kept constant at an intensity of 203-333 µE m^{-2} s^{-1}. Temperature was also kept constant at 13°C.

3 harvest frequencies were tested, every 4th, 8th, and 12th day respectively. There were 4 replicas pr. treatment, and the water used were pure RAS water coming from Hardingsmolt RAS facility.

Biomass were sampled by gently scaping off the attached biomass from the growth plates, by using a scraping tool. To limit the amount of water in the sample, the plates were first put in a 45- degree angle for 5 min, so water could easily run off. Then, plate laid horizontally for 5 min on aluminum foil to dry off even further. The biomass was then scraped off and transferred directly from the plate into a pre-marked and weighed 15 mL or 50mL centrifuge tube and weighed. All tubes were directly frozen down at -80°C awaiting further analyses.

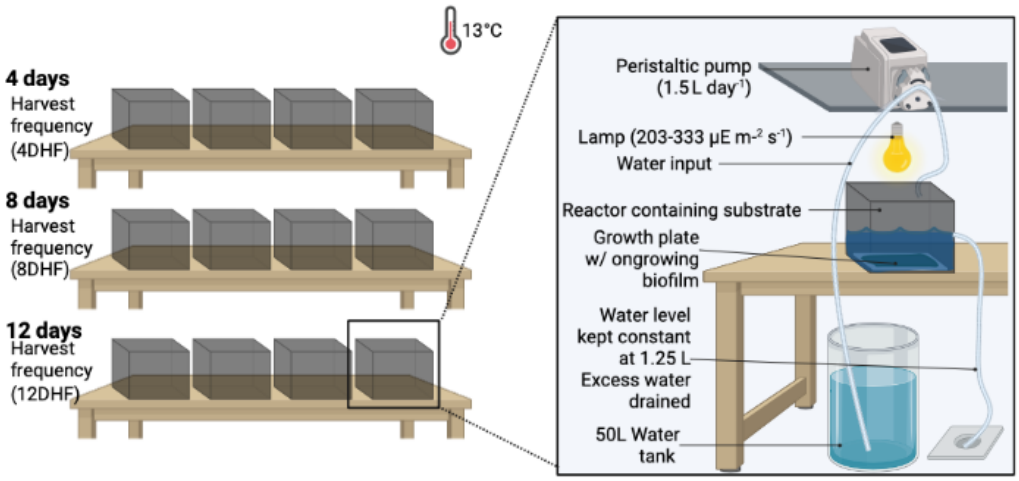

Figure 8: A visual overview of the setup of experiment IV. Schematic made using Biorender.

2.3.5 Hardingsmolt pilot study

Two reactor systems, one horizontal system and one vertical system, were placed on site at the Hardingsmolt RAS facility (Tørvikbygd, Hardanger). The specific design of the two systems is confidential, however the fundamental difference between them is the placement of the growth plates. For the horizontal system the growth plates were placed horizontally, and for the vertical system they were placed vertically. For both reactor systems the intake water was connected to the water sump after the mechanical drum filtration step. Biomass was sampled by gently scraping off the attached biomass on the growth plates, by using a scraping tool. Biomass was transferred directly from the plate into a pre-marked, weighed 50mL centrifuge tube, then weighed and frozen directly into -20°C. Samples were transported from Hardingsmolt RAS facility to Trondheim (NTNU Sealab), in a freezer bag to avoid thawing. All tubes were then directly frozen down at -80°C until further analyses.

2.4 Analyses

2.4.1 Water analysis ($P\text{-}PO_4^{3-}$, $N\text{-}NO_3^-$ and $N\text{-}NO_2^-$)

For all experiments, water samples were collected from the start water, and stored in the freezer until water analyses. Water samples were placed in a 4°C fridge and thawed overnight. All samples were filtrated through a syringe filter (25mm, 0.45µm). Samples were measured spectrophotometrically using an autoanalyzer (Flow Solution IV System, O.I. Analytical), following the Norwegian standard NS 4745 (1991), NS 4744 (1975) and NS 4724 (1984) for determination of $N\text{-}NO_3^- + N\text{-}NO_2^-$, $N\text{-}NO_2^-$ and $P\text{-}PO_4^{3-}$, respectively. All samples were diluted as the autoanalyzer has a maximum concentration of every compound within the standard curve. Dilutions were based on the water profile from measured values provided by Hardingsmolt RAS facility which are presented in Appendix B, Table B.1.

2.4.2 Biomass measurements

Biomass was measured to track growth (g m^{-2}) and to calculate SGR (day^{-1}) and productivity (g m^{-2} day^{-1}). However, different methods were used to measure biomass in the different experiments of this study. An overview of the methods used for biomass measurements in the respective experiment, are presented in Table 2. It should be noted that the biomass measurements for exp I and for the pilot study could not be used.

Table 2: Overview of the different methods utilized in this study to measure biomass.

Experiment	Biomass measurement method
Experiment I- effect of light intensity	Spectrophotometrically*
Experiment II- effect of silica addition	Inverse microscope pictures and ImageJ
Experiment III- effect of nutrient load	Inverse microscope pictures and ImageJ
Experiment IV- effect of harvest frequency	Gravimetrically (harvesting of biofilm by scraping)
Hardingsmolt pilot study	Gravimetrically (Harvesting of biofilm by scraping)*

*Biomass measurements could not be used

2.4.2.1 ImageJ

The image analyzing program ImageJ was used for biomass measurements in exp II and III, respectively. ImageJ analyzed the average% area of the pictures taken with the inverse microscope, using the code presented in Appendix D, Figure D.1 and Figure D.2. Values analyzed by ImageJ were manually investigated as the program in some cases can interpret 0% coverage as 100% coverage. 5 out of 334 values (exp II) and 23 out of 328 values (exp III) were therefore removed as outliers and not used in further analyses.

2.4.2.2 Conversion plot

When calculating growth rate and productivity for exp II and III, a conversion plot was used (Figure 9). As growth was measured taking pictures in the inverse microscope and analyzing them with the computer program ImageJ, average%area was converted to dry weight values. This was done to compare dry weight values measured gravimetrically in other experiments, to those derived from the picture taken with the inverse microscope. Additionally, dry weight (g m^{-2}) is a more intuitive unit compared to average%area. To establish the correlation between average%area samples and dry weight samples, a scatterplot showing average%area and corresponding average dry weight (g m^{-2}) for the same sample, were made. The corresponding dry weight to the microscope samples were conducted in an extended trial of exp II that was not a part of this study and is therefore not described. The best fitted line is shown by $Y = 0{,}2188*X + 26{,}42$, R^2 of the slope was 0,5329 and P- value of the slope was <0,0001, respectively. This equation was then used to convert average%area values to dry weight values.

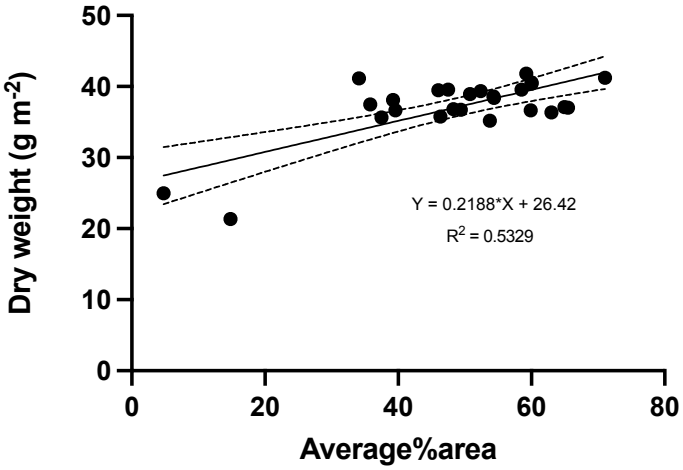

Figure 9: To establish the correlation between average%area samples and dry weight samples, a scatterplot showing average%area and corresponding average dry weight (g m^{-2}) for the same sample, was made. The best fitted line is shown by Y = 0,2188*X + 26,42, R^2 of the slope was 0,5329 and P- value of the slope was <0,0001, respectively. This information was utilized in the conversion of microscope data (average%area) to dry weight values.

2.4.3 Biofilm sample analyses

All biochemical analyses, conducted on the biofilm product, except freeze drying, used the same samples from exp IV. To limit the number of samples for biochemical analyses (due to time limitations and costs), four harvesting days were prioritized, where all four replicas were included, and specifics on this information are presented in Appendix C, Table C.1.

2.4.3.1 Freeze drying

Biomass samples in centrifuge tubes from exp II and IV, were freeze dried (Labconco, FreeZone® 70080 8L-50°C series) for 48 hours. The cap of the tubes was replaced with aluminum foil with small aeration holes. All samples were placed on the shelfs within the drying chamber of the freeze drier. Samples were then weighed directly after. Samples from exp IV were grinded using a mortar and pestle, flushed with N^2, and stored in centrifuge tubes at -80°C until further analyses. A detailed description of the methods for all conducted analyses are presented below.

2.4.3.2 Carbon and nitrogen content

Samples of freeze dried and grounded biofilm were weighed in tin-capsules using an ultra-micro scale (Mettler- Toledo), and the exact weight was recorded. Tin- capsules were folded on a carbon-free plate, using tweezers, and placed separately in a 96- microwell plate. The 96-well plate was then stored in a desiccator. Prior to the analysis, the samples were dried at 60°C overnight in a heating cabinet. CN- analysis was then performed using an elemental analyzer (Vario EL cube, ELEMENTAR AS, std. method) to determine C and N content in the individual capsules. Acetanilide and runin were used as standard solutions in this analysis. CN- analysis were conducted at TBS. N was used for calculations for estimated total crude protein (TCP).

2.4.3.3 Amino acid composition

The AA profile in freeze-dried ground biofilm product was analyzed by a HPLC system (Agilent Infinity 1260, Agilent Technologies) coupled to an on-line post-column derivatization module (Pinnacle PCX, Pickering laboratories, Mountain View, CA, USA), using nynhydrin (Trione) as a derivatizing reagent and Na+-ion exchange column (4.6 x 110 mm, 5 µm). 18 standard AA, NH_4^+ and taurin were quantified from standard curves measured with AA standards. Prior to the analysis, the samples were hydrolyzed in 6 M HCl containing 0.4% merkaptoethanol for 24 h at 110°C (HCl hydrolysis). Glutamine and asparagine were converted to glutamic and aspartic acid, respectively. Cystein was quantified as cystin (Cys-Cys). After filtration (micro filter), the pH was adjusted to 2.2 and the samples were further diluted with a citrate buffer (pH 2.2) for the HPLC analysis. All buffers, reagents, AA standards and the column were obtained from Pickering laboratories (Mountain View, CA, USA). HCl and merkaptoethanol were obtained from Sigma-Aldrich. The AA analyses were conducted at SINTEF Ocean, by Merete Selnes. The AA analysis was also used in calculations for estimating total protein (TP).

2.4.3.4 Total lipid content

Total lipid (TL) content were extracted using chloroform: methanol (2:1), following (Folch et al., 1957). 100mg freeze dried and grinded samples were weighed accurately into kimax- tubes using a Precisa 180A weight, and the exact weight was recorded. First, samples were moisturized with several drops of dH_2O. Then, samples were homogenized in 1.5mL methanol using Ultra Turrax T8 for 2 min. After the homogenization step, 3mL chloroform and 1.125mL 0,88% KCL (aq), were added. Samples were then vortexed for 10 seconds and thereafter centrifuged at 4000 rpm for 4 minutes at 4°C (Eppendorf centrifuge 5804 R). The organic phase was collected into pre-weighed tubes using a glass pipette. Remaining sample was reextracted by adding 2mL of chloroform and the step of vortex, centrifugating and collection of the organic phase was then repeated. Aliquots were taken out for each sample and dried under N_2, before being placed in a desiccator for 1 hour. TL were measured gravimetrically, and samples were then resolved in chloroform: methanol (2:1) to be stable for storing. TL analysis was conducted at NTNU Sealab, with lab training by Zdenka Bartosova.

2.4.3.5 Fatty acid composition

Analysis of FA composition were determined by converting FA components into FA methyl ester (FAME) using methanol, preceding gas chromatography (GC) analysis. 40ul lipid from each sample was transferred to a kimax tube and 1mL of $CHCl_3$ with ISTD (23:0) and 2mL 1% H_2SO_4: MeOH were added. Tubes were then flushed with N^2 and incubated on a heating block overnight. Samples were placed at room temperature and the lipids were washed out in three repeating steps using 5mL saturated NaCl and 6mL isooctane, samples were vortexed and centrifuged 4000 rpm for 3 min at 4°C (Eppendorf centrifuge 5804 R). The samples were then dried with N_2 and resolved in 200µL isooctane before being transferred into vials and analyzed using gas chromatography coupled to a flame ionization detector and mass spectrometer (Agilent 7890B). FA analysis was conducted at NTNU Sealab, with lab training by Zdenka Bartosova, she also ran the GC analysis.

2.4.3.6 Ash content

The ash content of the biofilm product was determined by combustion. Samples of freeze-dried and grounded biofilm (~100mg) were weighed in smaller pottery and glass containers and burned in a muffle furnace for five hours at 450 °C. Ash content in the samples was measured gravimetrically. Ash analysis was conducted at TBS.

2.5 Calculations

2.5.1 Specific growth rate

The specific growth rate (SGR) (day^{-1}) of the microalgae in exp II, III and IV, respectively, was calculated using Equation 4,

$$\text{Specific growth rate}(\mu) = \left(\frac{ln(m2) - ln(m1)}{t2 - t1}\right) \quad 4$$

where μ represents the SGR, m2 represents the final biomass concentration (t2) and m1 represents the initial biomass concentration (t1) (Krzemińska et al., 2014).

2.5.2 Productivty

The microalgae productivity (g m^{-2} day^{-1}) in exp II, III and IV, was calculated using Equation 5,

$$\text{Productivity}\left(\frac{kg}{day} \times \frac{1}{m2}\right) = \left(\frac{m2 - m1}{t2 - t1} \times \frac{1}{0{,}0025 \,/\, 0{,}0494\, m^2}\right) \quad 5$$

where m2 represents the final biomass concentration (at time point t2) and m1 represents the initial biomass concentration (at time point t1) (Krzemińska et al., 2014). The productivity was normalized to per. square meters (m^2) by multiplying by the square meters of the growth plates of the systems. For exp II and III the size of the growth was 0,0025m^2 and for exp IV the size of the growth plates for the reactor systems were 0,0494m^2, respectively.

2.5.3 Total protein estimate

2.5.3.1 Total crude protein content

TCP (mg g^{-1} DW) estimate was determined based on total N content. N content in the biomass product, obtain from the C-N analysis, were multiplied with a nitrogen-to-protein factor (6.25) to get a TCP estimate, as shown in Equation 6.

$$N_{Total} \times 6.25 \qquad 6$$

This calculation is based on two assumptions; 1) that the average N content in AA were found to be 16%, therefore giving the conversion factor of 6.25, and 2) that nearly all N in algal biomass is present as AA (Shuuluka et al., 2013).

2.5.3.2 Total water free amino acid content

The TP estimate was calculated based on the total content of AAs (mg g^{-1} DW). By subtracting the molar mass (M) of water from the molar mass of every AA, the dehydrated weight of the AA was determined. TP content was then estimated by multiplying the weight of the dehydrated AAs with the content of the corresponding AAs in the sample (mg g^{-1} DW), and is presented in Equation 7, where X indicates the specific AA.

$$\text{Protein content} = \frac{Amino\ acid\ X\ [M] - water\ [M]}{Amino\ acid\ X\ [M]} \times Amino\ acid\ X \left[\frac{mg}{g}\ DW\right] \qquad 7$$

The basis for this calculating is the fact that proteins are made of chains of AA bound by peptide bond containing a water molecule (OH-H) (Chang and Zhang, 2017). By subtracting the weight of the water molecule, an estimate of the TP content can be made.

2.6 Data treatment and statistical analysis

The visual representation of the data and statistical analysis were performed in Prism 9 (version: GraphPad Prism 9.5.0 (525)). All raw data were first treated in Microsoft Excel before transported to Prism. In Prism, all data was investigated with Normality test (Shapiro Wilk test), variance test (Levene`s test) and Identify outliers test. The identified outliers obtained by statistical test in Prism were then inspected manually before decided on being removed or not. Average%area data analyzed in ImageJ was also investigated manually as described in section 2.4.2.1 (ImageJ).

In exp II and exp III, as well as for the biochemical analyses of Hardingsmolt pilot study, Mann- Whitney test was used, comparing the means of two groups, assuming non-normally distributed data. Statistical analyses were performed at the 95% confidence level and a P- value <0.05 was considered statistically significant.

Kruskal-Wallis test, one- way analysis of variance (ANOVA) was used to analyze means of non-normally distributed data in-between multiple groups in exp IV, as well as for the biochemical analyses of exp IV. Dunn´s multiple comparisons test was used to compare the groups, when a significant difference was identified with Kruskal- Wallis test, to find which groups were significantly different from each other. Statistical analyses were performed at the 95% confidence level and a P- value <0.05 was considered statistically significant.

3 Results

3.1 Start water nutrient concentrations

The nutrient concentration (µg L^{-1}) (mean ± SD) in the start water coming from Hardingsmolt RAS facility for the four different experiments is presented in Table 3. Nutrients investigated were NO_2^-, NO_3^-, and phosphate (PO_4^{3-}). The water collected for exp I had the highest concentration of all three nutrients, while the water collected for exp II had the lowest concentrations of all the three nutrients. The water utilized in the Hardingsmolt pilot study was not characterized, as the pilot reactors were stationed at the facility for two months.

Table 3: Mean ± SD (for exp I and IV: n=4, for exp II and III: n=2) nutrient values for initial water samples in the four experiments. All water samples derived from Hardingsmolt RAS facility, however, collected at different timepoints which are specified in parenthesis for each experiment.

Nutrient	**Exp. I (Collected 31.01.2022)**	**Exp. II (Collected 01.03.2022)**	**Exp. III (Collected 02.05.2022)**	**Exp. IV (Collected 12.10.2022)**
Nitrite (NO_2^-) µg N L^{-1}	227.1± 6	127.3 ± 3	148.6 ± 2	104.2 ± 8
Nitrate (NO_3^-) mg N L^{-1}	36.0 ± 2	5.0 ± 0.06	32.6 ± 2	10.2 ± 4
Phosphate (PO_4^{3-}) µg P L^{-1}	2708 ± 182	774 ± 22	2023 ± 364	1245 ± 194

3.2 Growth of microalgae biofilm

3.2.1 Experiment I- Effect of light intensity

The experimental setup and growth measurements of exp I were customized to fit the cultivation of a planktonic culture, as vertical cell cultivations were used, and growth were measured spectrophotometrically. As the growth proved to be of benthic form, results from the growth measurements fit to measure planktonic growth (OD_{460nm}), are therefore not thrustable. Still, several important observations were made, and these are presented in Table 4. The microscopy picture shown in Figure 10 were taken from a sample of medium light condition under light microscope and it was found that diatoms where dominating the microalgae biofilm, this was also the case for high light conditions (Bonnefond, 2022).

Table 4: Results from exp I listed as observations. Numbers indicate the specific observation made.

	Observation
1	Cultivating a microalgal biofilm using the wastewater deriving from Hardingsmolt RAS facility were proven to be possible.
2	Benthic growth (photoautotrophs), a thin biofilm formed.
3	No growth (autotrophic or heterotrophic) in "No light" condition was observed.
4	Diatoms were dominating the microalgal consortium in medium and high light conditions, see Figure 10.

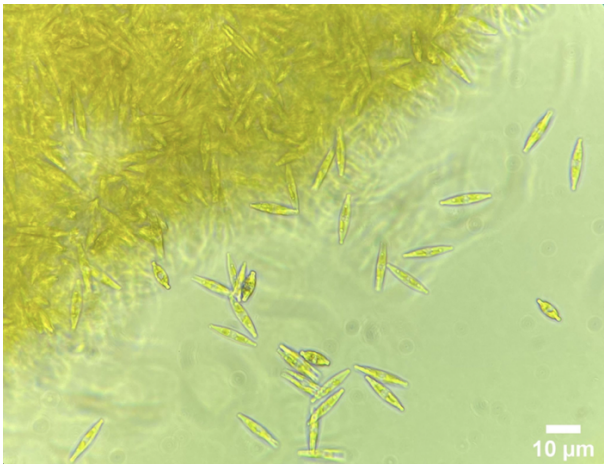

Figure 10: Picture taken from a biomass sample collected from medium light condition, using a light microscope at x40 magnification. Diatoms is dominating the consortium (Bonnefond, 2022).

3.2.2 Experiment II- Effect of silica addition

The average dry weight (g m^{-2}) (± SD, n=3) at each sampling day is plotted for both conditions (+Si and -Si) and are presented in Figure 11. There was a significant difference in dry weight biomass (g m^{-2}) between the two conditions (when comparing all harvestings throughout the experimental period) (Mann- Whitney test, P-value = 0.0002). Both conditions had 27 g m^{-2} at the start of the experiment (day 1), however the +Si condition had a dry weight value of 29 g m^{-2} at day 14, compared to the -Si conditions which had 28 g m^{-2} on the same day. The highest dry weight biomass obtained for the +Si condition was at day 7, reaching 30 g m^{-2}, and for the -Si condition it was 28 g m^{-2}, also at day 7.

The SGR (day^{-1}) (measured from day 1 to day 3) (± SD, n=3) and productivity (g m^{-2} day^{-1}) (measured from day 1 to day 6) (± SD, n=3) and their respective significant values (p- values) are presented in Table 5. The SGR of the +Si condition was 0.03 day^{-1}, and the -Si condition was significantly lower, being 0.002 day^{-1}. +Si condition had a productivity of 0.09 g m^{-2} day^{-1} and the -Si condition had a productivity of 0.04 g m^{-2} day^{-1}, however the significant threshold of 0.05 were not met for this observation. The microscope inspection revealed that the consortium in this experiment was dominated by diatoms in both conditions.

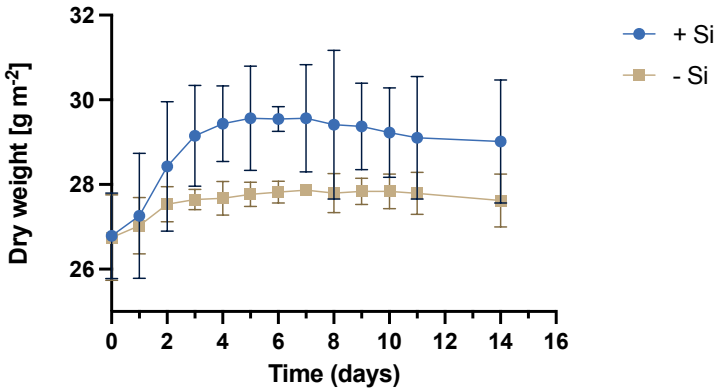

Figure 11: The dry weight (g m^{-2}) of the biofilm ± SD, n=3 harvested at different timepoints (day of harvest) for conditions: added silica (+Si) and no added silica (- Si).

Table 5: SGR (day^{-1}) and productivity (g m^{-2} day^{-1}) ± SD values, n=3, and significance values (p-values) for the two conditions: added silica (+Si) and no added silica (- Si).

Condition	**SGR [day^{-1}]**	**Significance (P- Value)**	**Productivity [g m^2 day^{-1}]**	**Significance (P- Value)**
+ Si	0.03 ± 0.00	0.01	0.09 ± 0.06	0.07
- Si	0.002 ± 0.00	0.00	0.04 ± 0.02	0.02

3.2.3 Experiment III- Effect of nutrient concentration

Dry weight (g m^{-2}) (± SD, n=3) was plotted as a function of time (harvest days) for both conditions and is presented in Figure 12. The initial (day 0) dry weight content was 26 g m^{-2} for both conditions and increased to 29 g m^{-2} for low nutrient condition on day 18, and 32 g m^{-2} for the high nutrient condition at day 18. There was a significant difference between the two conditions when comparing all harvestings throughout the experimental period (Mann- Whitney test, P-value = 0.004).

The SGR (day^{-1}) (± SD, n=4) (measured using values from day 4 to day 10) and productivity (g m^{-2} day^{-1}) (± SD, n=8) (measured using values from day 1 to day 18) and their respective significant values (p-values) are presented in Table 6. High nutrient condition had an SGR of 0.005 day^{-1}, whereas the low nutrient condition had an SGR of 0.01 day^{-1}, although neither value was significant ($p > 0.05$). The high nutrient condition had a productivity of 0.32 g m^{-2} day^{-1} and the condition with low nutrient had a productivity of 0.12 g m^{-2} day^{-1} ($p < 0.05$). The microscope inspection revealed that the consortium also in this experiment was dominated by diatoms in both conditions.

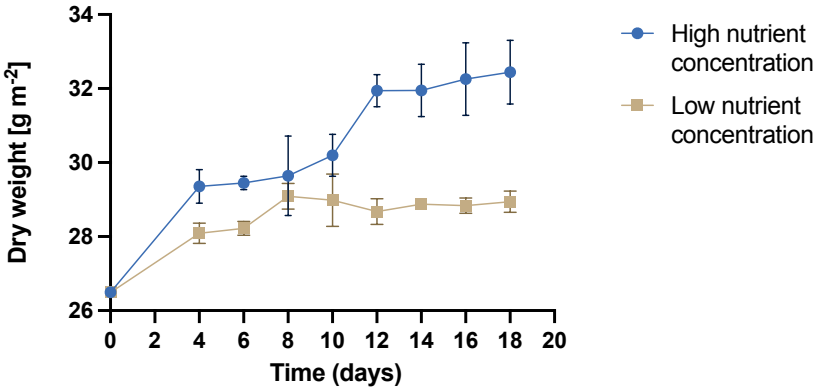

Figure 12: The dry weight (g m^{-2}) of the biofilm ± SD, n=3, harvested at different timepoints (day of harvest) for conditions high and low nutrient concentration.

Table 6: SGR (pr. day^{-1}) ± SD values, n=4 and productivity (g m^{-2} day^{-1}) ± SD values, n=8, and significance values (p-values) for the two conditions: high and low nutrient concentration.

Condition	**SGR [day^{-1}]**	**Significance (P- Value)**	**Productivity [g m^2 day^{-1}]**	**Significance (P- Value)**
High nutrient	0.005 ± 0.00	0.07	0.32 ± 0.04	<0.0001
Low nutrient	0.01 ± 0.00	0.17	0.12 ± 0.03	0.013

3.2.4 Experiment IV- Effect of harvest frequency

Figure 13 (A) shows the average biomass harvested throughout the experimental period for each condition. 4DHF had an average dry weight content of 6 g m^{-2}, the 8DHF had an average of 12 g $m^{-2,}$ and the 12DHF average was 22 g m^{-2}. Figure 13 (B) shows the dry weight values (g m^{-2}) in respect to the day of harvest. There was a significance difference between 4DHF and 12DHF (Kruskal- Wallis test, Dunn´s multiple comparisons test, P-value = 0.0049), however, there was no significant difference between 4DHF and 8DHF (Kruskal-Wallis test, Dunn´s multiple comparisons test, P-value = 0.07) nor between 8DHF and 12DHF (Kruskal- Wallis test, Dunn´s multiple comparisons test, P-value = >0.999). Significant differences are indicated with lowercase letters in Figure 13 (A).

The calculated productivity for the conditions tested were: 1.59 g m^{-2} day^{-1}, 1.50 g m^{-2} day^{-1}, and 1.80 g m^{-2} day^{-1} for the three conditions, 4DHF, 8DHF and 12DHF, respectively (Table 7). The productivity values are summarized in Table 7. All values were significant ($p < 0.05$). The microscope inspection revealed that the consortium also in this experiment was dominated by diatoms in both conditions.

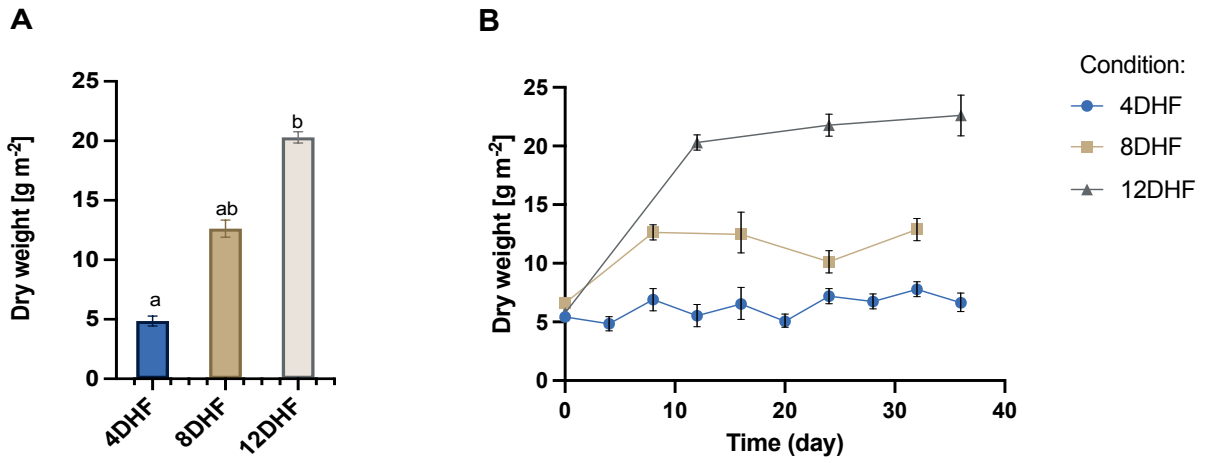

Figure 13: A: The average harvested biomass for the whole experimental period in dry weight (g m^{-2}) for the three conditions: 4DHF, 8DHF and 12DHF (± SD, n=4). Significant differences between groups are indicated with letters. **B**: Each day of harvest and the corresponding dry weight (g m^{-2}) value, shown for all three conditions.

Table 7: Productivity (g m^{-2} day^{-1}) ± SD, n=3, values for the three conditions: 4DHF, 8DHF and 12DHF.

Condition	**Productivity [g m^{-2} day^{-1}]**
4 days	1.59 ± 0.23
8 days	1.50 ± 0.14
12 days	1.80 ± 0.08

3.3 Characterization of biochemical composition of biofilm at different harvest frequencies

3.3.1 Carbon and nitrogen content

The carbon and nitrogen content (mg g^{-1} DW) (means ± SD, n=16) in the biofilm product from the three harvest frequency conditions was characterized and is presented in Figure 14. There was a significant difference observed in carbon content between the 4DHF and 8DHF (Kruskal- Wallis test, Dunn´s multiple comparison test, P-value = 0.0020) and the 4DHF and 12DHF conditions (Kruskal- Wallis test, Dunn´s multiple comparison test, P-Value = 0.0032).

There was a significant difference between the nitrogen content between the 4DHF and 12DHF condition (Kruskal- Wallis test, Dunn´s multiple comparison test, P-value = 0.0004), and between the 8DHF and the 4DHF (Kruskal- Wallis test, Dunn´s multiple comparison test, P-value = 0.0004).

The C/N ratio (mean ± SD, n=16) was also characterized, using weight (mg), and is presented in Table 8. No significant difference in C/N ratio was found between conditions (Kruskal- Wallis test, p-value = 0.1059).

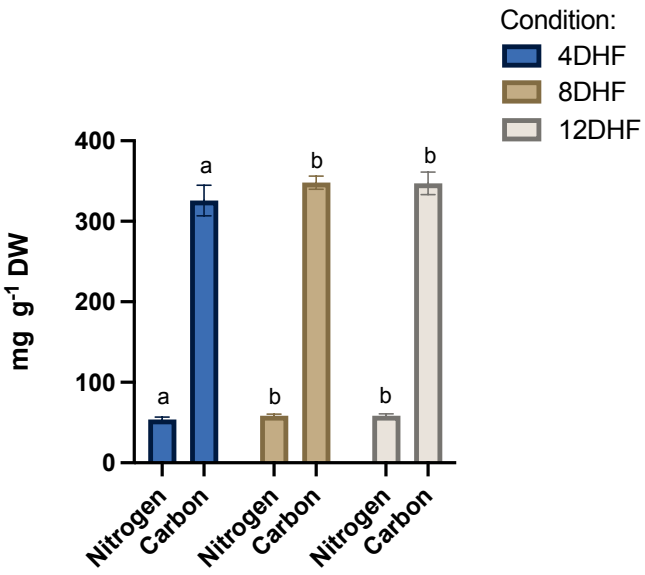

Figure 14: Carbon and nitrogen content of the biofilm product (mg g^{-1} DW) ± SD, n=16, in the three conditions: 4DHF, 8DHF and 12DHF. Significant differences are indicated with lowercase letters.

Table 8: The C/N ratio (mean ± SD, n=16) of the biofilm product for the three conditions: 4DHF, 8DHF and 12DHF. There were no significant differences between the three conditions.

	4DHF	**8DHF**	**12DHF**
C/N ratio	6.05 ± 0.04	5.97 ± 0.13	5.94 ± 0.07

3.3.2 Total protein content

Figure 15 (A) presents the estimated TCP (mg g^{-1} DW) (means ± SD, n=16). There was a significant difference in TCP content between 4DHF (335 mg g^{-1} DW) and 8DHF (362 mg g^{-1} DW) (Kruskal- Wallis test, Dunn´s multiple comparison test, P-Value = 0.0004), and between 4DHF and 12DHF (363 mg g^{-1} DW) (Kruskal- Wallis test, Dunn´s multiple comparison test, P-Value = 0.0004). No significant difference was found in TCP content between 8DHF and 12DHF (Kruskal- Wallis test P-value= >0.05).

The estimated TP (mg g^{-1} DW) (means ± SD, n=16) for the three conditions are presented in Figure 15 (B). No significant differences in TP content were found between conditions (Kruskal- Wallis test P-value= >0.05).

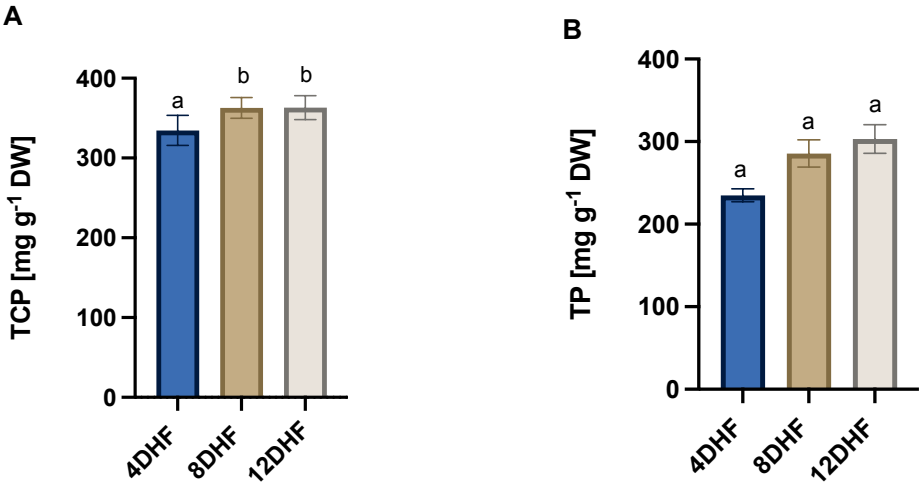

Figure 15: A: The estimated TP content in the biofilm product (mg g^{-1} DW) ± SD, n=16, in respect to the three conditions, based on the total N content in the biofilm, using a nitrogen-to-conversion factor (6.25). Significant differences are indicated with lowercase letters. **B**: The estimated TP content (mg g^{-1} DW) ± SD, n=16, in the biofilm product in respect to the three different conditions, based on the total content of water free AAs. There were no significant differences between conditions.

3.3.3 Amino acids composition

The AA composition (mg g^{-1} DW) (means ± SD, n=16) of the three groups: 4DHF, 8DHF, and 12DHF, were characterized. EAA are presented in Table 9 and non-essential amino (NEAA) acids in Table 10. The sum of EAA content ranged from 89 – 96 mg g^{-1} DW, however, no significant differences were found between conditions (Kruskal- Wallis test, P-value = >0.05). The sum NEAA contents ranged from 139 – 208 mg g^{-1} DW, where the 12DHF had a significant higher content, with a significant difference in sum NEAA contents between 4DHF and 12DHF (Kruskal- Wallis test, Dunn´s multiple comparison test, P-Value = 0.0426).

The most abundant EAA was leucine for all three conditions. Glutamic acid + Glutamine were the most abundant NEAA for the 4DHF, however for both 8DHF, and 12DHF, arginine was the most abundant. There was no significant difference in any of the individual AA contents between the conditions (Kruskal- Wallis test P-value= >0.05).

Table 9: EAA composition for the three conditions: 4DHF, 8DHF and 12DHF (mg g^{-1} DW) (means ± SD, n=16) and total EAA (mg g^{-1} DW) (means ± SD, n=16). There were no significant differences in sum EAA between conditions, nor in individual AA content.

Essential amino acid	**4DHF [mg g^{-1} DW]**	**8DHF [mg g^{-1} DW]**	**12DHF [mg g^{-1} DW]**
Histidine	3.4 ± 0.1	2.5 ± 0.1	2.6 ± 0.3
Isoleucine	11.2 ± 0.6	12.9 ± 0.5	13.5 ± 0.3
Leucine	19.1 ± 0.5	15.4 ± 0.5	16.4 ± 0.5
Lysine	19.6 ± 0.6	16.5 ± 0.4	29.0 ± 0.4
Methionine	4.8 ± 0.3	6.2 ± 0.5	6.3 ± 0.2
Phenylalanine	13.2 ± 0.4	10.5 ± 0.3	11.0 ± 0.4
Threonine	9.6 ± 0.5	11.3 ± 0.6	11.9 ± 0.8
Tryptophan	0.0 ± 0.0	1.1 ± 0.0	1.1 ± 0.0
Valine	15.4 ± 0.5	12.0 ± 0.3	15.6 ± 0.3
∑ Essential amino acids [mg g^{-1} DW]	96.3 ± 6.5[a]	88.6 ± 5.1[a]	94.7 ± 5.7[a]

Table 10: NEAA composition for the three conditions: 4DHF, 8DHF and 12DHF (mg g^{-1} DW) (means ± SD, n=16) and total NEAA (mg g^{-1} DW) (means ± SD, n=16). No significant difference in individual AA content was found between systems. However, there was a significant difference in the sum of NEAA between 4DHF and 12DHF. Significant differences are indicated with lowercase letters.

Non-essential amino	**4DHF [mg g^{-1} DW]**	**8DHF [mg g^{-1} DW]**	**12DHF [mg g^{-1} DW]**
Hydroxyproline	0.3 ± 0.1	4.0 ± 0.2	4.4 ± 0.2
Aspartic acid + Asparagine	15.7 ± 0.7	13.0 ± 0.7	13.4 ± 0.6
Serine	15.7 ± 0.7	19.8 ± 0.8	21.3 ± 0.7
Glutamic acid + Glutamine	30.6 ± 1.2	24.7 ± 0.7	25.8 ± 0.7
Proline	12.8 ± 0.7	11.9 ± 0.7	13.3 ± 0.7
Glycine	10.5 ± 0.4	11.4 ± 0.5	12.1 ± 0.4
Alanine	16.5 ± 0.8	11.7 ± 0.8	12.3 ± 0.7
Cystine (Cys-Cys)	3.5 ± 0.7	5.1 ± 0.5	5.4 ± 0.6
Tyrosine	7.8 ± 0.4	8.7 ± 0.2	9.1 ± 0.3
Hydroxylysine	0.3 ± 0.2	5.0 ± 0.30	5.0 ± 0.3
Arginine	24.9 ± 0.7	81.7 ± 2.0	86.2 ± 0.6
∑ Non-essential amino acids [mg g^{-1} DW]	138.6 ± 9.2[a]	197.1 ± 21.0[ab]	208.4 ± 22.2[b]

3.3.4 Total lipid content

The TL content (mg g^{-1} DW) (means ± SD, n=16) of the three conditions: 4DHF, 8DHF, and 12DHF ranged between 81 mg g^{-1} DW - 84 mg g^{-1} DW (Figure 16). There was no significant difference in TL content between conditions (Kruskal- Wallis test and Dunn´s multiple comparison test, P-value = >0.05).

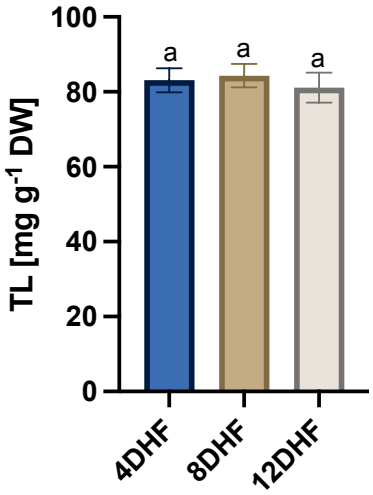

Figure 16: The TL content (mg g^{-1} DW) in respect to the biomass production obtained from the three conditions; 4DHF, 8DHF and 12DHF (mean ± SD, n=16). There were no significant differences between groups.

3.3.5 Fatty acid composition

The FA composition (% of total FA) (means ± SD, n=16) for the three groups, 4DHF, 8DHF, and 12DHF, is presented in Table 11. No significant difference in the individual FA content between the three conditions (Kruskal- Wallis test and Dunn´s multiple comparison test, P-value = >0.05). However, the most abundant FAs were C20:5 n-3 (EPA), C16:1 n-7 (Palmitoleic acid (PA)), C22:6 n-3 (DHA), C16:0 (Palmitic acid) and C14:0 (Myristic acid).

Table 11: FA distribution (% of total FA) (means ± SD, n=16) of the three conditions: 4DHF, 8DHF and 12DHF. There were no significant differences in individual FA between groups.

Fatty acid	4DHF [% of total FA]	8DHF [% of total FA]	12DHF [% of total FA]
C14:0 (Myristic acid)	5.7 ± 1.1	5.7 ± 1.4	16.4 ± 22.5
C16:0 (Palmitic acid)	8.3 ± 4.1	9.1 ± 5.5	10.4 ± 48.9
C16:1 n-7 (Palmitoleic acid)	25.2 ± 7.0	26.7 ± 9.1	27.8 ± 116.0
C16:1 n-9	0.3 ± 0.2	0.2 ± 0.1	0.2 ± 1.0
C16:1 n-5	0.8 ± 0.2	0.7 ± 0.1	0.68 ± 2.3
C16:2 n-6	0.9 ± 0.2	0.7 ± 0.2	0.6 ± 1.8
C16:2 n-4	2.1 ± 0.8	1.2 ± 0.6	1.7 ± 7.3
C16:3	3.0 ± 1.0	2.1 ± 0.4	1.9 ± 5.8
C16:4	4.2 ± 0.6	4.0 ± 0.5	3.6 ± 12.7
C18:0	0.3 ± 0.1	0.3 ± 0.1	0.3 ± 1.2
C18:1 n-9	1.1 ± 0.6	1.3 ± 0.8	1.6 ± 7.7
C18:1 n-7	0.8 ± .0.1	0.7 ± 0.2	0.7 ± 2.5
C18:2 n-6	1.6 ± 0.4	1.5 ± 0.4	1.4 ± 5.8
C18:3 n-3	0.8 ± 0.4	0.6 ± 0.3	0.44 ± 1.4
C18:4 n-3	1.0 ± 0.3	0.9 ± 0.3	10.0 ± 4.1
C20:4 n-6	0.6 ± 0.5	0.7 ± 0.5	10.0 ± 4.4
C20:5 n-3 (EPA)	28.2 ± 3.5	38.2 ± 4.6	27.0 ± 99.7
C22:6 n-3 (DHA)	4.7 ± 0.5	4.7 ± 0.7	4.1 ± 14.1
C24:1	0.0 ± 0.0	0.0 ± 0.0	0.0 ± 0.0

3.3.6 Ash content

Figure 17 shows the ash content in the three groups, 4DHF, 8DHF, and 12DHF. Due to limited sample volumes only one replicate could be analyzed (n=1), and no significant test to determine whether there are any significant differences between the treatments, could be conducted. Still, the 4DHF contained the highest ash content (284 mg g^{-1} DW), whereas the 12DHF contained the lowest ash content (248 mg g^{-1} DW), however it remains unknown whether these are significant differences.

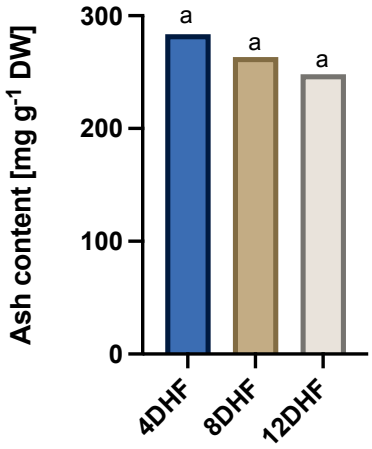

Figure 17: Ash content in the biofilm product (mg g^{-1} DW) (n=1), of the three conditions: 4DHF, 8DHF and 12DHF.

3.4 Characterization of biochemical composition of biofilm obtained from Hardingsmolt pilot study

3.4.1 Carbon and nitrogen content

The carbon and nitrogen content (mg g^{-1} DW) (means ± SD, n=4) in the biofilm product from the two reactor systems was characterized and is presented in Figure 18. There was no significant difference in carbon content between the horizontal system (324 mg g^{-1} DW) and the vertical system (46 mg g^{-1} DW) (Mann- Whitney test, P-Value = >0.05).

Also, there was no significant difference in nitrogen content between the horizontal system (53 mg g^{-1} DW) and the vertical system (46 mg g^{-1} DW) (Mann- Whitney test, P-Value = >0.05).

The C/N ratio (mean ± SD, n=4) was also characterized, using weight (mg), and is presented in Table 12. No significant difference in C/N ratio was found between conditions (Mann-Whitney test, p-value = 0.0571).

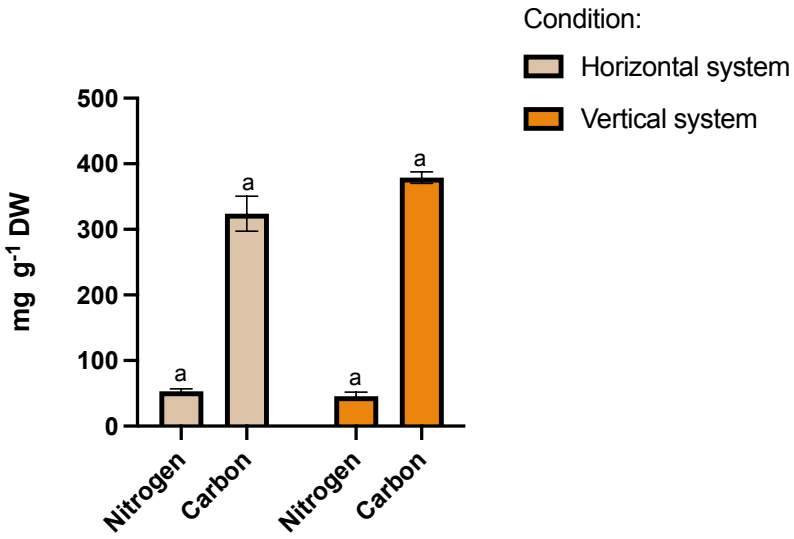

Figure 18: Carbon and nitrogen content (mg g^{-1} DW) (mean ± SD, n=4) of the biofilm product in the two conditions: horizontal and vertical system. There were no significant differences between the two systems.

Table 12: The C/N ratio (mean ± SD, n=4) of the biofilm product for the two conditions: horizontal and vertical system. There were no significant differences between the two systems.

	Horizontal system	**Vertical system**
C/N ratio	6.11 ± 0.12	8.42 ± 1.19

3.4.2 Total protein content

Figure 19 (A) presents the estimated TCP (mg g^{-1} DW) (means ± SD, n=4) in the two conditions, horizontal and vertical system. There was no significant difference in the TCP content between the two conditions (Mann- Whitney test, P-Value = >0.05).

The estimated TP (mg g^{-1} DW) (means ± SD, n=4) content in the two systems are presented in Figure 19 (B). The estimated TP content in the horizontal system were 210 mg g^{-1} DW and was significantly higher than the vertical system 184 mg g^{-1} DW (Mann-Whitney test, P-Value = 0.0001).

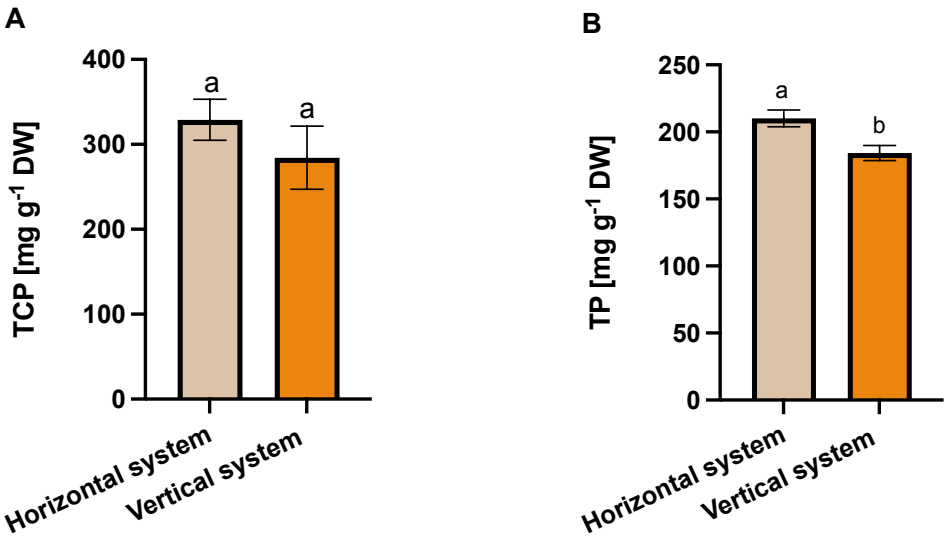

Figure 19: A: The estimated TCP content in the biofilm product (mg g^{-1} DW) ± SD, n=4, in respect to the two conditions. No significant differences between the two systems. **B**: The estimated TP content (mg g^{-1} DW) ± SD, n=4, in the biofilm product in respect to the two systems. Significant differences are indicated with lowercase letters.

3.4.3 Amino acid composition

AA composition (mg g^{-1} DW) (means ± SD, n=4) of the two pilot reactor systems were characterized and values of the EAA are presented in Table 13, and the NEAA are presented in Table 14. There was a significant difference in the sum EAA content between the two systems, where the sum EAA content was 89 mg g^{-1} DW for the horizontal system and 74 mg g^{-1} DW for the vertical system (Mann- Whitney test, P-Value = 0.0078). There was no significant difference in sum NEAA between systems (Mann- Whitney test, P-Value = >0.05).

Leucine was the most abundant EAA in both conditions, whereas Glutamic acid + Glutamine were the most abundant NEAA for both systems, however, no significant difference was found in any of the individual AA content between conditions (Mann- Whitney test, P-Value = >0.05).

Table 13: EAA composition for both two reactor systems, vertical and horizontal (mg g^{-1} DW) (means ± SD, n=4) and total EAA (mg g^{-1} DW) (means ± SD, n=4). No significant difference in individual AA content was found between systems. However, a significant difference between the sum of EAA was found and is indicated with lowercase letters.

Essential amino acids	**Horizontal system [mg g^{-1} DW]**	**Vertical system [mg g^{-1} DW]**
Histidine	3.0 ± 0.2	2.5 ± 0.8
Isoleucine	11.2 ± 0.3	8.9 ± 0.5
Leucine	16.3 ± 0.8	13.7 ± 0.5
Lysine	13.2 ± 0.8	11.4 ± 0.2
Methionine	5.1 ± 0.3	3.6 ± 0.4
Phenylalanine	14.2 ± 0.5	12.4 ± 0.5
Threonine	10.3 ± 0.5	8.5 ± 0.4
Tryptophan	0.0 ± 0.0	0.0 ± 0.0
Valine	15.6 ± 0.6	13.4 ± 0.4
∑ Essential amino acids [mg g^{-1} DW]	88.9 ± 5.5[a]	74.4 ± 4.8[b]

Table 14: NEAA composition for both reactor systems (means ± SD, n=4) and total NEAA (mg g^{-1} DW). No significant difference in individual AA content was found between systems, nor in the sum of NEAA.

Non-essential amino acids	**Horizontal system [mg g^{-1} DW]**	**Vertical system [mg g^{-1} DW]**
Hydroxyproline	0.3 ± 0.1	0.4 ± 0.1
Aspartic acid + Asparagine	15.9 ± 0.4	15.9 ± 0.6
Serine	15.0 ± 0.8	12.5 ± 0.2
Glutamic acid + Glutamine	23.5 ± 0.8	20.9 ± 0.5
Proline	11.9 ± 0.6	12.3 ± 0.5
Glycine	10.2 ± 0.3	8.1 ± 0.2
Alanine	15.7 ± 0.9	13.8 ± 0.9
Cystine (Cys-Cys)	2.9 ± 0.4	2.8 ± 0.2
Tyrosine	8.3 ± 0.4	5.9 ± 0.5
Hydroxylysine	0.4 ± 0.3	0.2 ± 0.1
Arginine	17.0 ± 1.4	17.1 ± 0.8
∑ Non-essential amino acids [mg g^{-1} DW]	121.2 ± 7.1[a]	109.9 ± 6.7[a]

3.4.4 Total lipid content

The TL content (mg g^{-1} DW) (means ± SD, n=4) in the biofilm product for the two pilot reactor systems, the vertical and horizontal reactor, respectively, is shown in Figure 20. There was no significant difference in TL content between the two conditions (Mann-Whitney test, P-Value = >0.05).

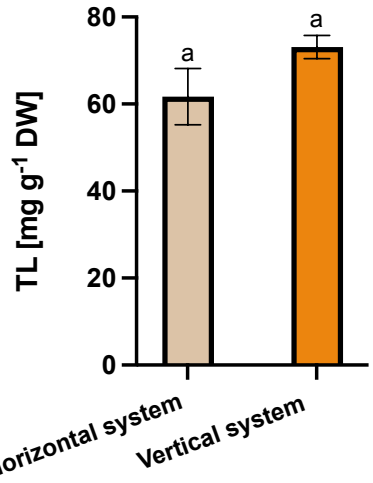

Figure 20: The TL content (mg g^{-1} DW) (mean ± SD, n=4) in respect to the biomass product obtained from two pilot systems placed at Hardingsmolt RAS facility: the horizontal system, and vertical system. There was no significant difference in the TL content between the two conditions.

3.4.5 Fatty acid composition

The FA composition (% of total FA) (mean ± SD, n=4) of the two reactor systems is presented in Table 15. No significant differences were found between the individual FA content between groups (Mann- Whitney test, P-value = >0.05), The most abundant FA was C16:1 n-7 (PA) for both systems. Other abundant FAs was C16:0 (Palmitic acid) and C20:5 n-3 (EPA).

Table 15: FA distribution (% of total FA) (means ± SD, n=4) of the biofilm cultivated in the horizontal and vertical system. No significant differences in individual FA content were observed.

Fatty acid	Horizontal system [% of total FA]	Vertical system [% of total FA]
C14:0	4.7 ± 0.8	5.1 ± 0.6
C16:0 (Palmitic acid)	12.2 ± 3.1	10.1 ± 5.3
C16:1 n-7 (Palmitoleic acid)	20.4 ± 3.3	32.5 ± 8.7
C16:1 n-9	0.5 ± 0.1	0.1 ± 0.0
C16:1 n-5	0.8 ± 0.1	0.5 ± 0.1
C16:2 n-6	1.3 ± 0.6	2.5 ± 0.9
C16:2 n-4	2.1 ± 0.4	0.8 ± 0.2
C16:3	5.5 ± 0.9	2.7 ± 1.0
C16:4	1.7 ± 0.4	0.8 ± 0.1
C18:0	3.1 ± 2.4	0.3 ± 0.1
C18:1 n-9	7.7 ± 6.0	4.6 ± 2.5
C18:1 n-7	3.1 ± 0.6	3.1 ± 1.6
C18:2 n-6	2.0 ± 1.1	1.1 ± 0.2
C18:3 n-3	1.4 ± 0.2	0.2 ± 0.0
C18:4 n-3	0.7 ± 0.1	0.3 ± 0.0
C20:4 n-6	3.8 ± 1.6	3.3 ± 0.7
C20:5 n-3 (EPA)	17.2 ± 3.2	17.2 ± 1.7
C22:6 n-3 (DHA)	2.5 ± 0.1	2.1 ± 0.3
C24:1	0.1 ± 0.1	0.1 ± 0.0

3.4.6 Ash content

Figure 21 shows the ash content in the two different reactor systems. Due to limited sample volumes only one replicate could be analyzed (n=1), no significant test to determine whether there are any significant differences between the treatments, could be conducted. Still, the horizontal system (308.8 mg g^{-1} DW) contains a higher ash content than the vertical system (205.2 mg g^{-1} DW), however it remains unknown whether these are significant differences.

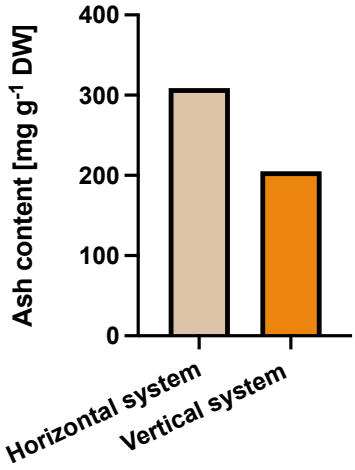

Figure 21: Ash content (mg g^{-1} DW, n=1), in the biomass product obtained from the two reactor systems, the horizontal and vertical system, respectively.

4 Discussion

4.1 Identifying optimal environmental conditions for cultivating microalgal biofilm

The experiments performed in this thesis aimed to identify optimal environmental parameters important for cultivating mixed community biofilm on RAS water. Benthic photoautotrophic organisms, which are dependent on light for photosynthesis, dominated the biofilm community. This was an important observation and indicated the essential role of light. As the setup and growth measurements for the light experiment were made to fit cultivation of a planktonic culture, the growth data measured could not be used to conclude on what light intensity were optimal for the growth system. Therefore, subsequent experiments used a high light intensity of 203-333 µE m^{-2} s^{-1}, assuming this would be better, knowing from the literature that the growth rate increases with the increasing light intensity up to a certain level, which is species dependent (Bialevich et al., 2022). Exceeding this limit might lead to photoinhibition, where the biomass production could be negatively affected (Lehmuskero et al., 2018). Light intensities far below the optimum might result in photo limitation, further reducing biomass production (Lehmuskero et al., 2018).

Microalgal biofilm cultivation presents challenges in distributing light due to varying exposure to photoinhibition and photo limitation across biofilm layers (Kesaano and Sims, 2014, Mantzorou and Ververidis, 2019). Several studies have found that high light intensities have induced photoinhibition in several microalgal strains. Li et. al. found that light inhibition was observed in *Chlorella kessleri* at light intensities above 120 µE $m^{-2}s^{-1}$ (Li et al., 2012). Yeh et. al. found that a light intensity of 82.8 µE m^{-2} s^{-1} induced photoinhibition in *Chlorella vulgaris* ESP-31. However, they also suggested that the light source itself may be important in addition to the light intensity, and that different algal strains can be adapted to different light intensities based on the conditions present at their natural light environment (Yeh et al., 2010). The high light intensity used in this study may have limited growth to some extent, by inducing a possible light inhibition. By repeating the experiments with modifications for benthic growth, the optimal light intensity for biofilm cultivation can be determined. From an industrial perspective, minimizing light intensity within the optimal range for the biofilm consortium is economically advantageous, considering the costs and energy requirements of high light intensities. Throughout this study, biofilms were cultivated under constant light, the photosynthetic assimilation were therefore continuous. Comparing this setup to a light-dark cycle would be interesting, particularly for industrial-scale applications aiming to further reduce energy consumption.

Through microscope analyses it was found that diatoms were dominating the microbial community, which raised the question of whether a possible silica limitation could appear, as silica is a macronutrient important for the diatom cell wall. A natural extension of the first experiment was therefore to investigate the effect of silica addition to the substrate (RAS water coming from Hardingsmolt).

Exp II demonstrated that an addition of silica gave a significant difference in biomass (g m^{-2}) when compared to the condition without silica addition (Figure 11). The +Si condition reached a plateau around day 5, before slightly decreasing and stabilizing again around day 10. The -Si condition had a modest increase and even though most biomass was harvested at day 7, it can be argued that a plateau was reached already at day 3.

The fact that both conditions reached a plateau quite early in the experiment, suggested that there was a factor limiting the growth. As the biofilm was cultivated in small cell cultivation flasks, without the medium being changed throughout the experimental period (14 days), the plateaus could be explained by a nutrient limitation. This was supported by the discovery that the RAS water was collected when the fish were on starvation (ahead of a treatment) and confirmed by the water analysis showing a lower nutrient content in this experiment compared to the others.

The growth for the exponential phase is significantly higher for the +Si condition compared to the -Si condition. This indicated that the silica concentration in the RAS water was limiting for the microalgae growth before a possible other limiting nutrient did. Silica was therefore highlighted as an important factor for the microalgal growth in this study and that the RAS water coming from Hardingsmolt had some limitations in terms of nutrients. From an industrial perspective, silica could be added to the RAS water before the photobioreactor, to elevate the productivity and growth. However, the primary focus is on the development of a system that can be sustained on nutrients present in the RAS water, without extensive modifications. Silica was therefore not added to the RAS water in the subsequent experiments.

In a RAS, there are always changes in the feeding rate and the fish is often going through starvation periods ahead of different treatments, such as vaccination or relocation. It was therefore interesting to investigate how the microalgal biofilm community handled different levels of nutrients. Exp III investigated the effects of high and low nutrient concentrations in the RAS water, simulating nutrient levels during normal/high feeding and starvation periods, respectively. The high nutrient condition obtained a significantly higher biomass (g m^{-2}) compared to the low nutrient condition (Figure 12). Also, the productivity was higher in the high nutrient condition than in the low nutrient condition (Table 6). As expected, a higher nutrient availability in the RAS water, provided a higher biomass yield compared to a lower nutrient availability.

The high nutrient condition had a relatively steep increase in biomass before the growth reached two plateaus, one around day 5, and the other around day 12. This can be explained by the different phases of biofilm formation; as the nutrient uptake typically undergo a slight decrease during the settling of the biofilm, which can explain the first plateau observed from day 5 (Mantzorou and Ververidis, 2019). As the biofilm matured, the nutrient uptake would typically increase again, in line with the growth, which was observed from day 8, as the growth entered another exponential growth phase (Mantzorou and Ververidis, 2019). Then a second plateau was reached around day 12, indicating that the biofilm growth might have reached the death phase, where the nutrient uptake decreases (Mantzorou and Ververidis, 2019). On the other hand, it can be argued that the growth only reached one plateau, as the last data points showed a slight increase towards the end of the experiment. Extending the experiment would have been interesting to determine if the growth continued to increase or if a death phase was indeed reached.

Another possible explanation to the two plateaus, is the rapid NH_4^+ uptake. Microalgae prefer NH_4^+ to other N forms as the reduction of NH_4^+ to organic matter has a much lower metabolic cost (Salbitani and Carfagna, 2021). The reduction of NO_3^- and/or NO_2^- has a higher metabolic cost due to being dependent on the reduction enzymes, nitrate reductase and nitrite reductase (Salbitani and Carfagna, 2021). The initial exponential growth phase until day 5 can be attributed to the rapid assimilation of NH_4^+, which depletes the available N source and leads to the first plateau. As the microalgae must generate reduction enzymes to further utilize NO_3^- and NO_2^-, the plateau persisted until day 7, after which another exponential growth phase occurred when alternative N sources could be utilized. While the second plateau around day 12 suggests a nutrient depletion, extending the experiment would have been beneficial to confirm whether it was a plateau or just the entrance of a steady state.

When investigating the low nutrient condition, the growth curve was more leveled compared to the high nutrient condition which had a steeper increase. The initial biomass was identical to the one for high nutrient, however, the low nutrient condition exhibited a more modest development, reaching a maximum biomass of 29 g m^{-2}, followed by a slight decrease and stabilization. The most natural explanation for the different patterns between the two conditions is nutrient depletion, as the initial biomass were identical, but the high nutrient condition achieved a higher total biomass compared to the low nutrient condition. Still, there were no signs of the biofilm in the low nutrient condition entering a death phase, suggesting the entrance of a steady state. This observation further emphasizes the need for a longer duration of the experiment to gather more conclusive results. Furthermore, it must be emphasized that if the biofilm community in fact entered a steady state, this is good news in an industrial perspective, as the biofilm can handle a quite low nutrient environment (low in a RAS perspective).

To determine the optimal harvest frequency for biomass productivity, three harvest frequencies were tested; 4, 8, and 12 days. In this study, harvest frequency refers to the time interval in which the microalgal biofilm got to grow before being harvested. The 8DHF were expected to reach the highest biomass productivity, based on literature from similar studies, showing that a harvest frequency between 6 – 7 days gave the highest biomass productivity (Gross et al., 2013, Boelee et al., 2014, Choudhary et al., 2017). Additionally, it was discussed whether the stress that would be inflicted on the biofilm with 4DHF, could disturb the growth development and result in a lower productivity. While in contrast, the low harvest frequency of 12DHF, was discussed to reach a biofilm thickness of which could lead to a possible photo limitation (Lehmuskero et al., 2018). In contrary to expectations, the 8DHF resulted in the lowest productivity, and the highest productivity was found in the 12DHF condition (Table 7). The results from exp IV indicated that a lower harvest frequency, gives a higher biomass productivity. When comparing the three different harvest frequencies, the only significant difference in dry weight (g m^{-2}) were found between the 4DHF and the 12DHF, and nearly a tripling in total biomass was observed between these two groups (Figure 13).

The 12DHF reaching the highest productivity can be attributed to various factors, including temperature. By comparing the temperature in the mentioned studies, the temperature ranged between 21°C to 25.5°C (Gross et al., 2013, Boelee et al., 2014). However, the experiment in this study were conducted in a temperature controlled room held at 13°C to simulate the RAS facility. Even though each species has its own optimal temperature, it is often found that an increasing temperature up to the optimal temperature, exponentially

increases the growth, and that this optimal temperature for microalgae often ranges between 20 – 30°C (Singh and Patidar, 2021, Reitan et al., 2021). Temperatures far below or above the optimum can cause the algae growth and activity to slow down and even stop, where low temperatures lowers the C assimilation for photosynthesis (Singh and Patidar, 2021). The temperature of 13°C in which the microalgal community in this study were growing, might have affected the growth in a way that slowed it down, which could explain why the longer harvest frequency of 12DHF resulted in a higher biomass content. From another point of view, the original temperature of the RAS water was also 13°C, at which it was kept throughout the experimental period. The species found in this RAS water, particularly those that thrive in it, are likely to possess a high tolerance for, if not an optimal adaptation to, the temperature of 13°C.

Regarding the light intensity in this experiment, it is uncertain if a photo limitation occurred in the biofilm, however it is clear that any potential photo limitation did not significantly restrict the growth. On the other hand, the high light intensity raises the question of whether the biofilm over the course of 12 days (for the condition with 12DHF) managed to develop protective mechanisms against the high light intensity. High light intensities can promote a more dense biofilm structure, and is described in literature as a way of protecting the cells from photo damage (Wang et al., 2021). The biofilm community in the 12DHF condition may have had sufficient time to undergo such structural changes as a response to the high light intensity, compared to the other frequencies. However, the microstructure of the biofilms was not investigated in this study, and it is important to note that this argument does not fully explain why the 4DHF showed higher productivity than the 8DHF. As for the other experiments conducted in this study, several factors and co—factors may be a part of the answer to these questions.

The pH was measured every harvest day throughout exp IV (presented in Appendix E, Table E.1). The flow-through reactor systems received a continuous supply of RAS water from a 50 L tank, which was refilled five times during the experimental period. Initially, the pH of the refilled water measured around 7, however, the pH quickly elevated a few days after being added. Throughout the experimental period, a consistently high pH of approximately 10 was measured for all three conditions. The high pH in the system can be explained by the removal of CO_2 by photosynthetic assimilation, in combination with no external addition of CO_2 sources (Larsdotter, 2006). The flow rate of 1.5L day^{-1} may have been insufficient for the size of the system, resulting in inadequate supply of CO_2 and nutrients to the biofilm. Furthermore, the absence of mixing in the systems limited the influx of CO_2 from the air. When the pH is high (>9), CO_2 is rapidly scavenged and the inorganic C is present as HCO_3^- and CO_3^-, with CO_3^- predominating (Vadlamani et al., 2017, Larsdotter, 2006). Most microalgae can utilize HCO_3^-, either directly or through the enzyme carbonic anhydrase (Larsdotter, 2006). Nevertheless, CO_3^- cannot be assimilated by microalgae, thus the low CO_2 availability act as a limitation for growth, as the photosynthetic rate decreases (Larsdotter, 2006). pH plays a crucial role in microalgal metabolism, growth and development, and a stable pH is therefore essential for biomass productivity (Qiu et al., 2017). The high pH observed in this study raises questions about its potential limitation on the growth of the microalgal biofilm. pH was not measured for any of the other experiments. As low biomass productivities were achieved in the other experiments as well, pH may have limited growth alone or in combination with other factors. Monitoring and controlling pH are vital for ensuring optimal growth in the aspect of cultivation.

Compared to small batch cultures (0.32 g m^{-2} day^{-1}), cultivating mixed community biofilm in flow through systems, yielded a higher biomass productivity (1.80 g m^{-2} day^{-1}) in this study. Still, when compared to similar studies it was found that the biomass productivity was quite low, as reported biomass productivities were between 10.92 g m^{-2} day^{-1} to 38.0 g m^{-2} day^{-1} (Rincon et al., 2017, Zhang et al., 2017, Wijihastuti et al., 2017). The low productivity in this study may be attributed to factors such as light intensity, pH, substrate, and system design, which may act alone or in combination to limit growth. Some of these factors such as pH, silica addition, cultivation methods, light and harvest frequency were investigated in this study, however further research is needed to better understand these and characterize other potential factors.

4.2 Biochemical composition of biofilm

In general, the biochemical profile of the three different harvest frequencies was quite similar. There was a significant difference in the TCP content between the 4DHF and 8DHF, and between 4DHF and 12DHF. However, no significant difference in the TP content was observed between the three conditions. These results indicated that the harvest frequency did not have a significant effect on the TP content of the mixed community biofilm product, however, a lower harvest frequency had a significant effect on the TCP content. Comparing the TP content to other studies conducted on microalgae it falls within the expected range, as reported levels range between 25 – 70% of dry cell weight (Rana and Prajapati, 2022, Zou et al., 2021, Zhang et al., 2017).

Also, the TCP and TP estimates showed relatively similar content values. This provides reliability to the methods used when estimating the protein content of the biofilm product, therefore providing reliability to the results as well. It can be argued that the TCP estimate is less accurate, as all N in the biofilm product is assumed to be protein, and does not take into account that some of the N can be found as e.g., free AAs, DNA and RNA (Lourenço et al., 1998). TP estimate can therefore be considered more accurate, as it is estimated from the actual measured AAs (total water free AA content).

No significant difference in sum EAA content among 4DHF, 8DHF and 12DHF was observed. However, there was a significant difference in the NEAA between 4DHF and 12DHF, indicating that a lower harvest rate gives a higher NEAA content. The higher total AA content associated with the 12DHF can be attributed to the higher TP content obtained under a lower harvest frequency. Lysine was the most abundant EAA for all conditions, which is promising looking from a feed perspective as lysine is highly important for protein synthesis in the fish, in addition to being a limiting EAA (Gatlin III et al., 2007, Berge et al., 1998). There was no significant differences found in the individual AA content between groups, which is expected as the AA profile between microalgal species has little variation (James et al., 1989).

No significant differences in TL content were found between conditions, as all values were approximately 80 mg g^{-1} DW. These results indicate that harvest frequency did not influence the TL content in this experiment. In conjugation with the high TP content, the low lipid content can be explained by the continuous replenishment of nutrients throughout the growth period. In nutrient- rich environments the C allocation tends to go toward metabolic processes such as protein synthesis and cell division (Allen et al., 2017). Consequently, a high protein content accompanied by a low TL content, is observed.

However, under nutrient depletion, particularly N- depletion, microalgae can adjust their C allocation priorities to shift towards lipid synthesis, as a response mechanism (Allen et al., 2017). This shift is often characterized as a decrease in protein content accompanied by an increase in lipid accumulation, over time (Allen et al., 2017). Previous studies by Levitan et. al (2015) and Rana et. al (2022) demonstrated these findings (Levitan et al., 2015, Rana and Prajapati, 2022). However, as there were no N limitations in this study, the TL content was low and even decreasing throughout the experiment, whilst the TP content remained relatively stable at a relatively high concentration (Appendix F, Figure F.1). In future research, investigating the biofilm under N- depletion would have been very interesting in a feed perspective.

TL values obtained in this study were low when compared to previous reported TL content in microalgae (Ye et al., 2018, Zou et al., 2021, Wang et al., 2019, Chauton et al., 2013). Furthermore, considering that the TL content remained the same for all three harvest frequencies, it would be more efficient, from an industrial perspective, to harvest every 4 days (4DHF) (only considering TL content). However, it is important to note that there might be other factors influencing this contemplation.

Looking at the FA profile, there was no significant difference in individual FAs, however, both DHA and EPA are present in all conditions. This is an interesting result in the context of feed, as EPA and DHA are especially important for growth and maintaining optimal immune function in fish, as well as for obtaining an EPA and DHA rich tissue, which is important for human consumption (Sargent et al., 2003, Taipale et al., 2016, Gladyshev et al., 2013). PA was the most abundant FA. PA has gained attention for its nutritional benefits for human health, such as e.g., increased insulin sensitivity (Maedler et al., 2003). Moreover, PA has also proven to be a good candidate for biodiesel production due to its favorable structural features (Zhou et al., 2017). The results indicate that by having a low harvest frequency, a higher FA content can be obtained.

The ash content was similar in the three conditions, however, as n=1 it was not possible to conduct any significant test. 4DHF had the highest ash content and 12DHF had the lowest. These results indicate that harvest rate did not influence the ash content in the microalgal biofilm to a great extent. As the biofilm were dominated by diatoms, a high level of ashes in the biofilm was expected, as the silica cell wall of diatoms will significantly add to the ash content (Hillman and Sims, 2020). It was also expected that since some RAS water with relatively high salinity (15 ppt) was present in the samples when freeze dried, a higher ash content could occur due to the amounts of salt in the water. This also means that the biofilm product will contain some salt, which will be important to investigate, especially regarding its relevance as a feed ingredient. The ash content is considered normal when compared to previous reported values (Gross and Wen, 2014, Roostaei et al., 2018).

Even though there are different designs of the two pilot reactors, they will not be compared independently or to each other. Detailed information regarding the designs of the reactor systems cannot be elaborated on due to confidentiality reasons, thus it was considered

irrelevant to treat them individually in this context. The average between the two systems was therefore used when comparing the pilot systems to the lab systems.

Overall, the biochemical profiles of the lab systems and the pilot systems were similar, and no significant differences were observed in any of the tested parameters. The similarities in the biochemical profile of the biomass obtained in the lab and in the on-site pilot reactors, provides a level of reliability and consistency to the results obtained in the lab. Additionally, it lends weight to the obtained results, as the lab results align with the results from the pilot study. This point is an important finding and a decisive factor for future research in this project.

4.3 Perspectives

With the rise in the use of RAS, there has been a corresponding increase in the demand for technologies that can remove NO_3^- and other inorganic nutrients from RAS water to prevent their discharge into the local environment (Ramli et al., 2020). The integration of microalgae in phototrophic bioreactors as part of RAS wastewater treatment has gained attention due to its capability to remove N and P from the RAS water while generating valuable biomass (Figure 4) (Wang et al., 2022). The present study demonstrated that cultivating microalgal biofilm on RAS water was possible, however, relatively low biomass productivities were obtained. It raised questions regarding the possible limitations of nutrients in the RAS water, as the addition of silica improved the biomass productivity. The pH and a limited CO_2 availability were also identified as potential challenges in the lab systems. Nevertheless, it remains uncertain whether these limitations and issues would persist in an on-site bioreactor in RAS, considering the high RAS water availability, thus the possibility of increasing the water flow to the reactor. The pH in RAS is not expected to be problematic, due to the pH being kept close to neutral for fish culture (Ramli et al., 2020). However, due to the highly aeriated RAS environment, the microalgae might face CO_2 deficiency (Ramli et al., 2020). A possible solution to this challenge can be the addition of CO_2 to the photobioreactor. This way, the microalgae get sufficient amounts CO_2 for photosynthesis, thus producing O_2 for the fish while simultaneously lowering the need for O_2 addition in the final steps of the RAS water treatment process (Ramli et al., 2020). Future research is needed to investigate the upscaling of such phototrophic biofilter and finding the most efficient, economical, and sustainable method to produce microalgal biomass while simultaneously purifying RAS wastewater. Additionally, evaluating the bioremediation potential of the biofilm consortia in the photobioreactor is crucial in calculating the effectiveness of the water recycling in RAS and for optimalization of the water treatment process, thus, being an important economic factor as well.

One of the objectives of the biochemical investigation was to evaluate the nutritional relevance of the biofilm product as a potential feed ingredient for e.g., Atlantic salmon (*Salmo salar*). As feed presents the largest expense to the industry, finding new sustainable feed ingredients is important (Ansari et al., 2021). Looking at the dietary requirements of Atlantic salmon, The Food and Agriculture Organization of the United Nations (FAO) have defined nutritional requirements for each life stage (FAO, 2021). Juvenile Atlantic salmon require approximately 40-50% crude protein and 18-30 % crude lipids, along with well-balanced AA and EFA profiles (FAO, 2021). In the present study, the

biofilm product reached a TP content of around 27 % DW and a TL content of 8.3 % DW, which is lower than the FAO requirements in both cases. However, the biofilm product might remain an interesting candidate as a supplement in fish feed, as there are other benefits related to microalgae beyond protein and lipid contents. Lysine, methionine, arginine and threonine are limiting AAs in salmon when marine resources in the feed (fishmeal) is replaced with plant derived protein (FAO, 2021). Cysteine is also an important AA for digestibility of protein, fat and starch (Nordrum et al., 2000). If the biofilm product were to replace fishmeal in the future, it is therefore important that these AAs are present at relatively high levels. For the mentioned AAs, there is an increasing concentration with a decreasing harvest rate in this study, meaning that the 12DHF had the highest concentration of the mentioned AAs. However, all conditions were in the required range according to the levels of recommendation (FAO, 2021). The requirements for specific FA such as DHA and EPA are met by the content in the biofilm product, with a DHA content of 0.7% DW and 4.2% DW EPA content (Average of the three conditions) (FAO, 2021). Furthermore, analyzing carbohydrates, PO_4^{3-}, pigments, vitamins, and minerals, while ensuring the absence of potential hazardous components, is essential for further assessment of the nutritional value of the biofilm product, regarding the relevance as a feed substitute. Therefore, further research is necessary both to confirm the values obtained in this study, as well as investigating the biochemical composition and potential further.

5 Conclusions

The present study has demonstrated the successful cultivation of microalgal biofilm using water obtained from Recirculating Aquaculture Systems (RAS) (Hardingsmolt AS). Light was underlined as an important factor as the biofilm community consisted of photoautotrophic organisms. The addition of silica, high nutrient concentration in the substrate, and a 12 day harvest frequency was found to increase the productivity and biomass yield substantially. It was also found that cultivating the microalgal biofilm in flow through reactor systems, gave a higher productivity when compared to batch systems. The highest biomass productivity achieved was found in the photoautotrophic flow through systems using unmodified RAS water and a 12 day harvest frequency (1.80 g m^{-2} day^{-1}).

The biochemical profiles of the biofilm product under the effect of different harvest frequencies (4 days, 8 days, 12 days) were characterized. In general, the three conditions had similar biochemical compositions. A significant difference was found in the total crude protein content, where the 12 day harvest frequency had the highest total crude protein content (363 mg g^{-1} DW). Additionally, a significant difference was found in sum non-essential amino acid content where the 12 day harvest frequency had the highest content (208 mg g^{-1} DW). For the other tested parameters, the three groups remained similar. Lysine, arginine, and glutamic acid + glutamine was the most abundant amino acids. The valuable polyunsaturated fatty acids, eicosapentaenoic acid (EPA), and docosahexaenoic acid (DHA), as well as palmitoleic acid was present in all conditions. This biochemical characterization indicates that the microalgal biofilm product obtained in this study presents an interesting potential fish feed candidate.

When comparing the lab-scale systems to the on-site pilot reactors, no significant differences in biochemical content was observed. These findings provide a level of reliability and depth to the results obtained in the laboratory, which is important for future research on this project.

This study was a great first step towards understanding the microalgal community growing on RAS water and its integration in phototrophic bioreactors as part of RAS wastewater treatment. Results on the valuable biochemical profile of the biofilm product also provides an interesting contribution to its potential as feedstock. Further research to comprehensively explore all aspects of the biofilm community and enhance biomass production and productivity is needed and recommended.

References

AHMAD, A., W. HASSAN, S. & BANAT, F. 2022. An overview of microalgae biomass as a sustainable aquaculture feed ingredient: food security and circular economy. *Bioengineered,* 13**,** 9521-9547.

AHMED, N. & TURCHINI, G. M. 2021. Recirculating aquaculture systems (RAS): Environmental solution and climate change adaptation. *Journal of Cleaner production,* 297**,** 126604.

ALHATTAB, M., KERMANSHAHI-POUR, A. & BROOKS, M. S.-L. 2019. Microalgae disruption techniques for product recovery: influence of cell wall composition. *Journal of Applied Phycology,* 31**,** 61-88.

ALLEN, J. W., DIRUSSO, C. C. & BLACK, P. N. 2017. Carbon and acyl chain flux during stress-induced triglyceride accumulation by stable isotopic labeling of the polar microalga Coccomyxa subellipsoidea C169. *Journal of Biological Chemistry,* 292**,** 361-374.

ALMEIDA, D. B., MAGALHÃES, C., SOUSA, Z., BORGES, M. T., SILVA, E., BLANQUET, I. & MUCHA, A. P. 2021. Microbial community dynamics in a hatchery recirculating aquaculture system (RAS) of sole (Solea senegalensis). *Aquaculture,* 539**,** 736592.

ANDERSEN, R. A. 2013. The microalgal cell. *Handbook of microalgal culture: applied phycology and biotechnology***,** 1-20.

ANSARI, F. A., GULDHE, A., GUPTA, S. K., RAWAT, I. & BUX, F. 2021. Improving the feasibility of aquaculture feed by using microalgae. *Environmental Science and Pollution Research,* 28**,** 43234-43257.

AZIZI, M., MOTESHAFI, H. & HASHEMI, M. 2020. A novel CO2 steady feeding based on the pH steady strategy data in the Haematococcus pluvialis cultivation to maximize the cell growth and carbon bio-sequestration. *Bioresource Technology,* 314**,** 123752.

BADIOLA, M., BASURKO, O., PIEDRAHITA, R., HUNDLEY, P. & MENDIOLA, D. 2018. Energy use in recirculating aquaculture systems (RAS): a review. *Aquacultural engineering,* 81**,** 57-70.

BERGE, G. E., SVEIER, H. & LIED, E. 1998. Nutrition of Atlantic salmon (Salmo salar); the requirement and metabolic effect of lysine. *Comparative Biochemistry and Physiology Part A: Molecular & Integrative Physiology,* 120**,** 477-485.

BERNER, F., HEIMANN, K. & SHEEHAN, M. 2015. Microalgal biofilms for biomass production. *Journal of applied phycology,* 27**,** 1793-1804.

BIALEVICH, V., ZACHLEDER, V. & BIŠOVÁ, K. 2022. The effect of variable light source and light intensity on the growth of three algal species. *Cells,* 11**,** 1293.

BOELEE, N., JANSSEN, M., TEMMINK, H., TAPARAVIČIŪTĖ, L., KHIEWWIJIT, R., JÁNOSKA, A., BUISMAN, C. & WIJFFELS, R. 2014. The effect of harvesting on biomass production and nutrient removal in phototrophic biofilm reactors for effluent polishing. *Journal of applied phycology,* 26**,** 1439-1452.

BONGIORNO, T., FOGLIO, L., PROIETTI, L., VASCONI, M., MORETTI, V., LOPEZ, A., CARMINATI, D., GALAFAT, A., VIZCAÍNO, A. & FERNÁNDEZ, F. A. 2022. Hydrolyzed microalgae from biorefinery as a potential functional ingredient in Siberian sturgeon (A. baerii Brandt) aquafeed. *Algal Research,* 62**,** 102592.

BONNEFOND, H. 2022. Microalgae microscope analysis *In:* RØNNING, L. (ed.).

CHANG, S. K. & ZHANG, Y. 2017. Protein analysis. *Food analysis***,** 315-331.

CHAUTON, M. S., OLSEN, Y. & VADSTEIN, O. 2013. Biomass production from the microalga Phaeodactylum tricornutum: nutrient stress and chemical composition in exponential fed-batch cultures. *Biomass and bioenergy,* 58**,** 87-94.

CHAUTON, M. S., REITAN, K. I., NORSKER, N. H., TVETERÅS, R. & KLEIVDAL, H. T. 2015. A techno-economic analysis of industrial production of marine microalgae as a

source of EPA and DHA-rich raw material for aquafeed: Research challenges and possibilities. *Aquaculture,* 436**,** 95-103.
CHEAH, Y. T. & CHAN, D. J. C. 2021. Physiology of microalgal biofilm: a review on prediction of adhesion on substrates. *Bioengineered,* 12**,** 7577-7599.
CHEN, B., WAN, C., MEHMOOD, M. A., CHANG, J.-S., BAI, F. & ZHAO, X. 2017. Manipulating environmental stresses and stress tolerance of microalgae for enhanced production of lipids and value-added products–A review. *Bioresource technology,* 244**,** 1198-1206.
CHEN, S., LING, J. & BLANCHETON, J.-P. 2006. Nitrification kinetics of biofilm as affected by water quality factors. *Aquacultural engineering,* 34**,** 179-197.
CHIARAMONTI, D., PRUSSI, M., CASINI, D., TREDICI, M. R., RODOLFI, L., BASSI, N., ZITTELLI, G. C. & BONDIOLI, P. 2013. Review of energy balance in raceway ponds for microalgae cultivation: Re-thinking a traditional system is possible. *Applied Energy,* 102**,** 101-111.
CHOUDHARY, P., PRAJAPATI, S. K., KUMAR, P., MALIK, A. & PANT, K. K. 2017. Development and performance evaluation of an algal biofilm reactor for treatment of multiple wastewaters and characterization of biomass for diverse applications. *Bioresource technology,* 224**,** 276-284.
DA SILVA, V. P., VAN DER WERF, H. M., SPIES, A. & SOARES, S. R. 2010. Variability in environmental impacts of Brazilian soybean according to crop production and transport scenarios. *Journal of environmental management,* 91**,** 1831-1839.
DALIRIAN, N., NAJAFABADI, H. A. & MOVAHEDIRAD, S. 2021. Surface attached cultivation and filtration of microalgal biofilm in a ceramic substrate photobioreactaor. *Algal Research,* 55**,** 102239.
DAVIDSON, J., GOOD, C., WILLIAMS, C. & SUMMERFELT, S. T. 2017. Evaluating the chronic effects of nitrate on the health and performance of post-smolt Atlantic salmon Salmo salar in freshwater recirculation aquaculture systems. *Aquacultural engineering,* 79**,** 1-8.
DEVI, N. D., CHAUDHURI, A. & GOUD, V. V. 2022. Algae biofilm as a renewable resource for production of biofuel and value-added products: A review. *Sustainable Energy Technologies and Assessments,* 53**,** 102749.
ESTEVAM, B. R., PINTO, L. F. R. & FREGOLENTE, L. V. 2022. Growth and Metabolite Production in Chlorella sp.: Analysis of Cultivation System and Nutrient Reduction. *BioEnergy Research***,** 1-12.
FANESI, A., PAULE, A., BERNARD, O., BRIANDET, R. & LOPES, F. 2019. The Architecture of Monospecific Microalgae Biofilms. *Microorganisms,* 7**,** 352.
FAO. 2021. *Atlantic Salmon - Nutritional requirements* [Online]. Available: https://www.fao.org/fishery/affris/species-profiles/atlantic-salmon/nutritional-requirements/en/ [Accessed 20.04 2023].
FJELLHEIM, A. J., HESS-ERGA, O.-K., ATTRAMADAL, K.J.K., VADSTEIN, O. 2017. "Recycling of water in hatchery production - Background Booklet for courses in recycling technology for hatchery production"
FLEMMING, H.-C. & WINGENDER, J. 2010. The biofilm matrix. *Nature reviews microbiology,* 8**,** 623-633.
FOLCH, J., LEES, M. & SLOANE STANLEY, G. H. 1957. A simple method for the isolation and purification of total lipids from animal tissues. *J biol Chem,* 226**,** 497-509.
GATLIN III, D. M., BARROWS, F. T., BROWN, P., DABROWSKI, K., GAYLORD, T. G., HARDY, R. W., HERMAN, E., HU, G., KROGDAHL, Å. & NELSON, R. 2007. Expanding the utilization of sustainable plant products in aquafeeds: a review. *Aquaculture research,* 38**,** 551-579.
GAUTHIER, M., SENHORINHO, G. & SCOTT, J. 2020. Microalgae under environmental stress as a source of antioxidants. *Algal Research,* 52**,** 102104.
GLADYSHEV, M. I., SUSHCHIK, N. N. & MAKHUTOVA, O. N. 2013. Production of EPA and DHA in aquatic ecosystems and their transfer to the land. *Prostaglandins & other lipid mediators,* 107**,** 117-126.

GROSS, M., HENRY, W., MICHAEL, C. & WEN, Z. 2013. Development of a rotating algal biofilm growth system for attached microalgae growth with in situ biomass harvest. *Bioresource technology,* 150**,** 195-201.
GROSS, M. & WEN, Z. 2014. Yearlong evaluation of performance and durability of a pilot-scale revolving algal biofilm (RAB) cultivation system. *Bioresource technology,* 171**,** 50-58.
GÜR, T. M. 2022. Carbon dioxide emissions, capture, storage and utilization: Review of materials, processes and technologies. *Progress in Energy and Combustion Science,* 89**,** 100965.
HILLMAN, K. M. & SIMS, R. C. 2020. Struvite formation associated with the microalgae biofilm matrix of a rotating algal biofilm reactor (RABR) during nutrient removal from municipal wastewater. *Water Science and Technology,* 81**,** 644-655.
HU, Y., XIAO, Y., LIAO, K., LENG, Y. & LU, Q. 2021. Development of microalgal biofilm for wastewater remediation: from mechanism to practical application. *Journal of Chemical Technology & Biotechnology,* 96**,** 2993-3008.
JAMES, C., AL-HINTY, S. & SALMAN, A. 1989. Growth and ω3 fatty acid and amino acid composition of microalgae under different temperature regimes. *Aquaculture,* 77**,** 337-351.
JIA, F., PENG, S., GREEN, J., KOH, L. & CHEN, X. 2020. Soybean supply chain management and sustainability: A systematic literature review. *Journal of Cleaner Production,* 255**,** 120254.
KATARZYNA, L., SAI, G. & SINGH, O. A. 2015. Non-enclosure methods for non-suspended microalgae cultivation: literature review and research needs. *Renewable and sustainable energy reviews,* 42**,** 1418-1427.
KESAANO, M. & SIMS, R. C. 2014. Algal biofilm based technology for wastewater treatment. *Algal Research,* 5**,** 231-240.
KHAN, M. I., SHIN, J. H. & KIM, J. D. 2018. The promising future of microalgae: current status, challenges, and optimization of a sustainable and renewable industry for biofuels, feed, and other products. *Microbial cell factories,* 17**,** 1-21.
KILBANE, J. J. 2022. Shining a light on wastewater treatment with microalgae. *Arabian Journal for Science and Engineering,* 47**,** 45-56.
KOUZUMA, A. & WATANABE, K. 2015. Exploring the potential of algae/bacteria interactions. *Current Opinion in Biotechnology,* 33**,** 125-129.
KRZEMIŃSKA, I., PAWLIK-SKOWROŃSKA, B., TRZCIŃSKA, M. & TYS, J. 2014. Influence of photoperiods on the growth rate and biomass productivity of green microalgae. *Bioprocess and biosystems engineering,* 37**,** 735-741.
LARSDOTTER, K. 2006. Wastewater treatment with microalgae-a literature review. *Vatten,* 62**,** 31.
LEHMUSKERO, A., CHAUTON, M. S. & BOSTRÖM, T. 2018. Light and photosynthetic microalgae: A review of cellular-and molecular-scale optical processes. *Progress in oceanography,* 168**,** 43-56.
LEVITAN, O., DINAMARCA, J., ZELZION, E., LUN, D. S., GUERRA, L. T., KIM, M. K., KIM, J., VAN MOOY, B. A., BHATTACHARYA, D. & FALKOWSKI, P. G. 2015. Remodeling of intermediate metabolism in the diatom Phaeodactylum tricornutum under nitrogen stress. *Proceedings of the National Academy of Sciences,* 112**,** 412-417.
LI, T., WANG, W., YUAN, C., ZHANG, Y., XU, J., ZHENG, H., XIANG, W. & LI, A. 2020. Linking lipid accumulation and photosynthetic efficiency in Nannochloropsis sp. under nutrient limitation and replenishment. *Journal of Applied Phycology,* 32**,** 1619-1630.
LI, Y., ZHOU, W., HU, B., MIN, M., CHEN, P. & RUAN, R. R. 2012. Effect of light intensity on algal biomass accumulation and biodiesel production for mixotrophic strains Chlorella kessleri and Chlorella protothecoide cultivated in highly concentrated municipal wastewater. *Biotechnology and bioengineering,* 109**,** 2222-2229.
LIU, J., WU, Y., WU, C., MUYLAERT, K., VYVERMAN, W., YU, H.-Q., MUÑOZ, R. & RITTMANN, B. 2017. Advanced nutrient removal from surface water by a consortium of attached microalgae and bacteria: a review. *Bioresource Technology,* 241**,** 1127-1137.

LOURENÇO, S. O., BARBARINO, E., MARQUEZ, U. M. L. & AIDAR, E. 1998. Distribution of intracellular nitrogen in marine microalgae: basis for the calculation of specific nitrogen-to-protein conversion factors. *Journal of Phycology,* 34**,** 798-811.
LUO, A., WANG, F., SUN, D., LIU, X. & XIN, B. 2022. Formation, development, and cross-species interactions in biofilms. *Frontiers in Microbiology,* 12**,** 3982.
MA, S., HUANG, Y., ZHANG, B., ZHU, X., XIA, A., ZHU, X. & LIAO, Q. 2023. Comprehensive modeling and predicting light transmission in microalgal biofilm. *Journal of Environmental Management,* 326**,** 116757.
MAEDLER, K., OBERHOLZER, J., BUCHER, P., SPINAS, G. A. & DONATH, M. Y. 2003. Monounsaturated fatty acids prevent the deleterious effects of palmitate and high glucose on human pancreatic β-cell turnover and function. *Diabetes,* 52**,** 726-733.
MALCORPS, W., KOK, B., VAN 'T LAND, M., FRITZ, M., VAN DOREN, D., SERVIN, K., VAN DER HEIJDEN, P., PALMER, R., AUCHTERLONIE, N. A. & RIETKERK, M. 2019. The sustainability conundrum of fishmeal substitution by plant ingredients in shrimp feeds. *Sustainability,* 11**,** 1212.
MANTZOROU, A. & VERVERIDIS, F. 2019. Microalgal biofilms: A further step over current microalgal cultivation techniques. *Science of the Total Environment,* 651**,** 3187-3201.
MEIER, L., VILCHEZ, C., CUARESMA, M., TORRES-ARAVENA, Á. & JEISON, D. 2022. Effect of pH Change on the Microalgae-Based Biogas Upgrading Process. *Applied Sciences,* 12**,** 12194.
NAGARAJAN, D., VARJANI, S., LEE, D.-J. & CHANG, J.-S. 2021. Sustainable aquaculture and animal feed from microalgae–nutritive value and techno-functional components. *Renewable and Sustainable Energy Reviews,* 150**,** 111549.
NORDRUM, S., KROGDAHL, Å., RØSJØ, C., OLLI, J. J. & HOLM, H. 2000. Effects of methionine, cysteine and medium chain triglycerides on nutrient digestibility, absorption of amino acids along the intestinal tract and nutrient retention in Atlantic salmon (Salmo salar L.) under pair-feeding regime. *Aquaculture,* 186**,** 341-360.
OLAIZOLA, M. & GREWE, C. 2019. Commercial microalgal cultivation systems. *Grand challenges in algae biotechnology.* Springer.
PIRES, J., ALVIM-FERRAZ, M., MARTINS, F. & SIMÕES, M. 2013. Wastewater treatment to enhance the economic viability of microalgae culture. *Environmental Science and Pollution Research,* 20**,** 5096-5105.
PRABU, E., FELIX, S., FELIX, N., AHILAN, B. & RUBY, P. 2017. An overview on significance of fish nutrition in aquaculture industry. *International Journal of Fisheries and Aquatic Studies,* 5**,** 349-355.
PREENA, P. G., REJISH KUMAR, V. J. & SINGH, I. S. B. 2021. Nitrification and denitrification in recirculating aquaculture systems: the processes and players. *Reviews in Aquaculture,* 13**,** 2053-2075.
QIU, R., GAO, S., LOPEZ, P. A. & OGDEN, K. L. 2017. Effects of pH on cell growth, lipid production and CO2 addition of microalgae Chlorella sorokiniana. *Algal research,* 28**,** 192-199.
RAMLI, N. M., VERRETH, J., YUSOFF, F. M., NURULHUDA, K., NAGAO, N. & VERDEGEM, M. C. 2020. Integration of algae to improve nitrogenous waste management in recirculating aquaculture systems: A review. *Frontiers in Bioengineering and Biotechnology,* 8**,** 1004.
RANA, M. S. & PRAJAPATI, S. K. 2022. Mixotrophic microalgal-biofilm reactor augmenting biomass and biofuel productivity. *Bioresource Technology,* 356**,** 127306.
REITAN, K. I., ØIE, G., JØRGENSEN, H. & WANG, X. 2021. Chemical composition of selected marine microalgae, with emphasis on lipid and carbohydrate production for potential use as feed resources. *Journal of Applied Phycology,* 33**,** 3831-3842.
RINCON, S. M., ROMERO, H. M., AFRAMEHR, W. M. & BEYENAL, H. 2017. Biomass production in Chlorella vulgaris biofilm cultivated under mixotrophic growth conditions. *Algal research,* 26**,** 153-160.
ROJAS-TIRADO, P., PEDERSEN, P. B., VADSTEIN, O. & PEDERSEN, L.-F. 2019. Microbial dynamics in RAS water: Effects of adding acetate as a biodegradable carbon-source. *Aquacultural Engineering,* 84**,** 106-116.

ROOSTAEI, J., ZHANG, Y., GOPALAKRISHNAN, K. & OCHOCKI, A. J. 2018. Mixotrophic microalgae biofilm: a novel algae cultivation strategy for improved productivity and cost-efficiency of biofuel feedstock production. *Scientific reports,* 8**,** 12528.
ROSLI, S. S., KADIR, W. N. A., WONG, C. Y., HAN, F. Y., LIM, J. W., LAM, M. K., YUSUP, S., KIATKITTIPONG, W., KIATKITTIPONG, K. & USMAN, A. 2020. Insight review of attached microalgae growth focusing on support material packed in photobioreactor for sustainable biodiesel production and wastewater bioremediation. *Renewable and Sustainable Energy Reviews,* 134**,** 110306.
ROUND, F. E., CRAWFORD, R. M. & MANN, D. G. 1990. *Diatoms: biology and morphology of the genera*, Cambridge university press.
RUANE, J., SONNINO, A. & AGOSTINI, A. 2010. Bioenergy and the potential contribution of agricultural biotechnologies in developing countries. *Biomass and Bioenergy,* 34**,** 1427-1439.
RUSSELL, C., RODRIGUEZ, C. & YASEEN, M. 2021. High-value biochemical products & applications of freshwater eukaryotic microalgae. *Science of The Total Environment***,** 151111.
SALBITANI, G. & CARFAGNA, S. 2021. Ammonium utilization in microalgae: A sustainable method for wastewater treatment. *Sustainability,* 13**,** 956.
SARGENT, J. R., TOCHER, D. R. & BELL, J. G. 2003. The lipids. *Fish nutrition***,** 181-257.
SCHNURR, P. J. & ALLEN, D. G. 2015. Factors affecting algae biofilm growth and lipid production: A review. *Renewable and Sustainable Energy Reviews,* 52**,** 418-429.
SEVIOUR, T., DERLON, N., DUEHOLM, M. S., FLEMMING, H.-C., GIRBAL-NEUHAUSER, E., HORN, H., KJELLEBERG, S., VAN LOOSDRECHT, M. C., LOTTI, T. & MALPEI, M. F. 2019. Extracellular polymeric substances of biofilms: Suffering from an identity crisis. *Water research,* 151**,** 1-7.
SHAH, M. R., LUTZU, G. A., ALAM, A., SARKER, P., KABIR CHOWDHURY, M., PARSAEIMEHR, A., LIANG, Y. & DAROCH, M. 2018. Microalgae in aquafeeds for a sustainable aquaculture industry. *Journal of applied phycology,* 30**,** 197-213.
SHUULUKA, D., BOLTON, J. J. & ANDERSON, R. J. 2013. Protein content, amino acid composition and nitrogen-to-protein conversion factors of Ulva rigida and Ulva capensis from natural populations and Ulva lactuca from an aquaculture system, in South Africa. *Journal of applied phycology,* 25**,** 677-685.
SINGH, G. & PATIDAR, S. 2021. Development and applications of attached growth system for microalgae biomass production. *BioEnergy Research,* 14**,** 709-722.
SINGH, J. & SAXENA, R. C. 2015. An introduction to microalgae: diversity and significance. *Handbook of marine microalgae.* Elsevier.
STANLEY, N. R. & LAZAZZERA, B. A. 2004. Environmental signals and regulatory pathways that influence biofilm formation. *Molecular microbiology,* 52**,** 917-924.
STEVČIĆ, Č., PULKKINEN, K. & PIRHONEN, J. 2019. Screening of microalgae and LED grow light spectra for effective removal of dissolved nutrients from cold-water recirculating aquaculture system (RAS) wastewater. *Algal Research,* 44**,** 101681.
SUTHERLAND, I. W. 2001. The biofilm matrix–an immobilized but dynamic microbial environment. *Trends in microbiology,* 9**,** 222-227.
SWANSON, D., BLOCK, R. & MOUSA, S. A. 2012. Omega-3 fatty acids EPA and DHA: health benefits throughout life. *Advances in nutrition,* 3**,** 1-7.
SZATKOWSKA, A. B. & PAULSRUD, B. 2014. The anammox process for nitrogen removal from wastewater–achievements and future challenges. *Innsendte Artikler,* 2**,** 186-194.
TAIPALE, S., VUORIO, K., STRANDBERG, U., KAHILAINEN, K., JÄRVINEN, M., HILTUNEN, M., PELTOMAA, E. & KANKAALA, P. 2016. Lake eutrophication and brownification downgrade availability and transfer of essential fatty acids for human consumption. *Environment International,* 96**,** 156-166.
TANG, H., CHEN, M., SIMON NG, K. & SALLEY, S. O. 2012. Continuous microalgae cultivation in a photobioreactor. *Biotechnology and bioengineering,* 109**,** 2468-2474.

TOM, A. P., JAYAKUMAR, J. S., BIJU, M., SOMARAJAN, J. & IBRAHIM, M. A. 2021. Aquaculture wastewater treatment technologies and their sustainability: A review. *Energy Nexus,* 4**,** 100022.

TOSSAVAINEN, M., LAHTI, K., EDELMANN, M., ESKOLA, R., LAMPI, A.-M., PIIRONEN, V., KORVONEN, P., OJALA, A. & ROMANTSCHUK, M. 2019a. Integrated utilization of microalgae cultured in aquaculture wastewater: wastewater treatment and production of valuable fatty acids and tocopherols. *Journal of Applied Phycology,* 31**,** 1753-1763.

TOSSAVAINEN, M., LAHTI, K., EDELMANN, M., ESKOLA, R., LAMPI, A.-M., PIIRONEN, V., KORVONEN, P., OJALA, A. & ROMANTSCHUK, M. 2019b. Integrated utilization of microalgae cultured in aquaculture wastewater: wastewater treatment and production of valuable fatty acids and tocopherols. *Journal of Applied Phycology,* 31**,** 1753-1763.

VADLAMANI, A., VIAMAJALA, S., PENDYALA, B. & VARANASI, S. 2017. Cultivation of microalgae at extreme alkaline pH conditions: a novel approach for biofuel production. *ACS Sustainable Chemistry & Engineering,* 5**,** 7284-7294.

VAN RIJN, J. & BARAK, Y. Denitrification in recirculating aquaculture systems: from biochemistry to biofilters. The Second International Conference on Recirculating Aquaculture, Cooperative Extension/Sea Grant, Virginia Tech, Blacksburg, Virginia, 1998. 179-187.

VILLAR-NAVARRO, E., GARRIDO-PÉREZ, C. & PERALES, J. A. 2021. The potential of different marine microalgae species to recycle nutrients from recirculating aquaculture systems (RAS) fish farms and produce feed additives. *Algal Research,* 58**,** 102389.

VILLAR-NAVARRO, E., RUIZ, J., GARRIDO-PÉREZ, C. & PERALES, J. A. 2022. Microalgae biotechnology for simultaneous water treatment and feed ingredient production in aquaculture. *Journal of Water Process Engineering,* 49**,** 103115.

WALTER K. DODDS, M. R. W. 2010. *Freshwater Ecology*.

WANG, C., TAN, Y., ZHU, L., ZHOU, C., YAN, X., XU, Q., RUAN, R. & CHENG, P. 2022. The intrinsic characteristics of microalgae biofilm and their potential applications in pollutants removal—A review. *Algal Research***,** 102849.

WANG, J.-H., ZHUANG, L.-L., XU, X.-Q., DEANTES-ESPINOSA, V. M., WANG, X.-X. & HU, H.-Y. 2018. Microalgal attachment and attached systems for biomass production and wastewater treatment. *Renewable and Sustainable Energy Reviews,* 92**,** 331-342.

WANG, X., FOSSE, H. K., LI, K., CHAUTON, M. S., VADSTEIN, O. & REITAN, K. I. 2019. Influence of nitrogen limitation on lipid accumulation and EPA and DHA content in four marine microalgae for possible use in aquafeed. *Frontiers in Marine Science,* 6**,** 95.

WANG, Y., JIANG, Z., LAI, Z., YUAN, H., ZHANG, X., JIA, Y. & ZHANG, X. 2021. The self-adaption capability of microalgal biofilm under different light intensities: Photosynthetic parameters and biofilm microstructures. *Algal Research,* 58**,** 102383.

WIJIHASTUTI, R. S., MOHEIMANI, N. R., BAHRI, P. A., COSGROVE, J. J. & WATANABE, M. M. 2017. Growth and photosynthetic activity of Botryococcus braunii biofilms. *Journal of applied phycology,* 29**,** 1123-1134.

WOLD, P.-A., HOLAN, A. B., ØIE, G., ATTRAMADAL, K., BAKKE, I., VADSTEIN, O. & LEIKNES, T. O. 2014. Effects of membrane filtration on bacterial number and microbial diversity in marine recirculating aquaculture system (RAS) for Atlantic cod (Gadus morhua L.) production. *Aquaculture,* 422**,** 69-77.

YAO, S., LYU, S., AN, Y., LU, J., GJERMANSEN, C. & SCHRAMM, A. 2019. Microalgae–bacteria symbiosis in microalgal growth and biofuel production: a review. *Journal of applied microbiology,* 126**,** 359-368.

YE, Y., HUANG, Y., XIA, A., FU, Q., LIAO, Q., ZENG, W., ZHENG, Y. & ZHU, X. 2018. Optimizing culture conditions for heterotrophic-assisted photoautotrophic biofilm growth of Chlorella vulgaris to simultaneously improve microalgae biomass and lipid productivity. *Bioresource Technology,* 270**,** 80-87.

YEH, K. L., CHANG, J. S. & CHEN, W. M. 2010. Effect of light supply and carbon source on cell growth and cellular composition of a newly isolated microalga Chlorella vulgaris ESP-31. *Engineering in Life Sciences,* 10**,** 201-208.
YUAN, H., ZHANG, X., JIANG, Z., WANG, X., WANG, Y., CAO, L. & ZHANG, X. 2020. Effect of light spectra on microalgal biofilm: Cell growth, photosynthetic property, and main organic composition. *Renewable Energy,* 157**,** 83-89.
ZHANG, B., LI, W., GUO, Y., ZHANG, Z., SHI, W., CUI, F., LENS, P. N. & TAY, J. H. 2020. Microalgal-bacterial consortia: from interspecies interactions to biotechnological applications. *Renewable and Sustainable Energy Reviews,* 118**,** 109563.
ZHANG, Q., LIU, C., LI, Y., YU, Z., CHEN, Z., YE, T., WANG, X., HU, Z., LIU, S. & XIAO, B. 2017. Cultivation of algal biofilm using different lignocellulosic materials as carriers. *Biotechnology for biofuels,* 10**,** 1-16.
ZHOU, W., WANG, H., CHEN, L., CHENG, W. & LIU, T. 2017. Heterotrophy of filamentous oleaginous microalgae Tribonema minus for potential production of lipid and palmitoleic acid. *Bioresource technology,* 239**,** 250-257.
ZHUANG, L.-L., YU, D., ZHANG, J., LIU, F.-F., WU, Y.-H., ZHANG, T.-Y., DAO, G.-H. & HU, H.-Y. 2018. The characteristics and influencing factors of the attached microalgae cultivation: A review. *Renewable and Sustainable Energy Reviews,* 94**,** 1110-1119.
ZOU, X., XU, K., CHANG, W., QU, Y. & LI, Y. 2021. A novel microalgal biofilm reactor using walnut shell as substratum for microalgae biofilm cultivation and lipid accumulation. *Renewable Energy,* 175**,** 676-685.
ZUCCARO, G., YOUSUF, A., POLLIO, A. & STEYER, J.-P. 2020. Microalgae cultivation systems. *Microalgae cultivation for biofuels production***,** 11-29.

Appendix A: Coordinates on cell cultivation flask for inverse microscope

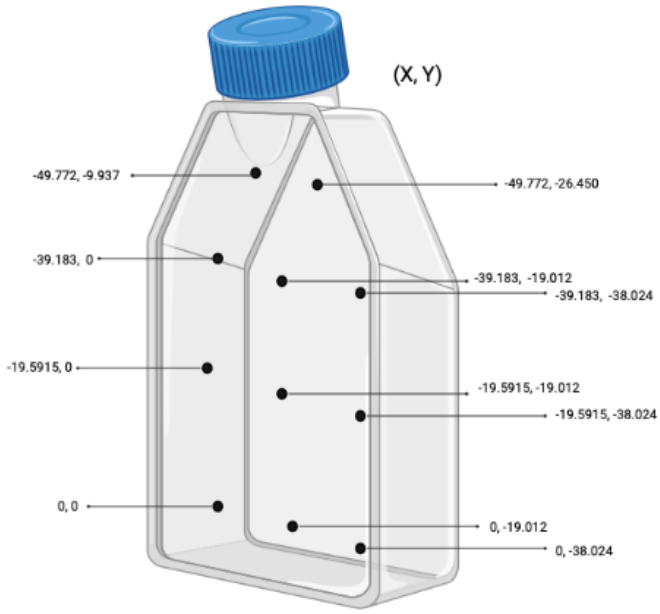

Figure A. 1: Pictures were taken at 11 specific coordinates (x,y) on the cell cultivation flask (indicated by arrows), using an inverse microscope (200x magnification), during growth measurements of exp II and exp III.

Appendix B: Hardingsmolt RAS water characteristics and dilutions

Table B. 1: The values of NO_2^- and NO_3^-N measured at facility the day of collection (dates are indicated), for exp I, II, and IV. When the water for exp III was collected the fish was on starvation and the facility did not carry out any water measurements.

Nutrient	**Exp. I** **(Collected 31.01.2022)**	**Exp. II** **(Collected 01.03.2022)**	**Exp. III** **(Collected 02.05.2022)**	**Exp. IV** **(Collected 12.10.2022)**
Nitrite (NO_2^-) mg L^{-1}	0.6	Fish was on starvation	0.06	0.15
Nitrate (N-NO_3^-) mg L^{-1}	56.0	Fish was on starvation	56.0	15.6

Appendix C: Harvest days for biochemical analyses

Table C. 1: Overview of all harvest days for exp IV in respect to the date, absolute time, and relative time in the timeline of the experiment. Harvest days used for biochemical analysis is highlighted by bold fonts.

	Inoculation and acclimation			**Experimental period**									
Date	17/10	24/10	25/10	4/11	8/11	12/11	16/11	20/11	24/11	28/11	2/12	6/12	10/12
Absolute time	0	7	8	14	18	22	26	30	34	38	42	46	50
Relative time	-14	-7	-6	0	4	8	12	16	20	24	28	32	36
4 days harvest frequency	NH	NH	NH	**H**	H	H	**H**	H	H	**H**	H	H	**H**
8 days harvest frequency	NH	NH	NH	**H**		**H**		H		**H**		**H**	
12 days harvest frequency	NH	NH	NH	**H**			**H**			**H**			**H**

NH **=** No Harvest**, H =**Harvest and used for biochemical analyses**,** H **=** Harvest but not used for biochemical analyses.

Appendix D: ImageJ analysis code

```
//https://imagej.nih.gov/ij/docs/menus/analyze.html
//https://imagej.nih.gov/ij/docs/menus/process.html#find

PictureDirectory = "C:\\Users\\johan\\Desktop\\Masteroppgave\\Eksp 1.1\\Eksp 1.1 - Cultivation flask
(starvation)\\20220325_ImageJ\\Silica\\"; //lieu d'enregistrement des images.
liste = getFileList(PictureDirectory);
setBatchMode(false); //travailler sans affichage = true


for (i=0; i<(liste.length); i++){
        if (endsWith(liste[i], ".jpg")){
                NamePicture= liste[i];
                NamePictureAdress = PictureDirectory + liste[i] ; //ouverture des images
                open (NamePictureAdress); //ouverture des images

                setOption("BlackBackground", false);
                run("8-bit");

                run("Sharpen");

                run("Find Edges");


                run("Convert to Mask");
                setAutoThreshold("Default");

                run("Close-");

                run("Analyze Particles...", "size=5-Infinity show=Masks clear include summarize"); //
valeur initiale size = 3000

        }
}
```

Figure D. 1: Code used in Image J to analyze the Average %Area of the pictures taken with Inverse microscope (200x magnification). The code was provided by Hubert Bonnefond.

```
//https://imagej.nih.gov/ij/docs/menus/analyze.html
//https://imagej.nih.gov/ij/docs/menus/process.html#find

PictureDirectory = "C:\\Users\\johan\\Desktop\\Masteroppgave\\Eksp 1.2 -
Cultivation flask\\Analyze\\"; //lieu d'enregistrement des images.
liste = getFileList(PictureDirectory);
setBatchMode(false); //travailler sans affichage = true
for (i=0; i<(liste.length); i++){
      if (endsWith(liste[i], ".jpg")){
            NamePicture= liste[i];
            NamePictureAdress = PictureDirectory + liste[i] ; //ouverture des
images
            open (NamePictureAdress); //ouverture des images
            setOption("BlackBackground", false);
            run("8-bit");
            run("Sharpen");
            run("Find Edges");
            run("Convert to Mask");
            setAutoThreshold("Default");
            run("Close-");
            run("Analyze Particles...", "size=5-Infinity show=Masks clear
include summarize"); //valeur initiale size = 3000}}
```

Figure D. 2: Code used in Image J to analyze the Average %Area of the pictures taken with Inverse microscope (200x magnification). The code was provided by Hubert Bonnefond.

Appendix E: pH values for experiment IV- Effect of harvest frequency

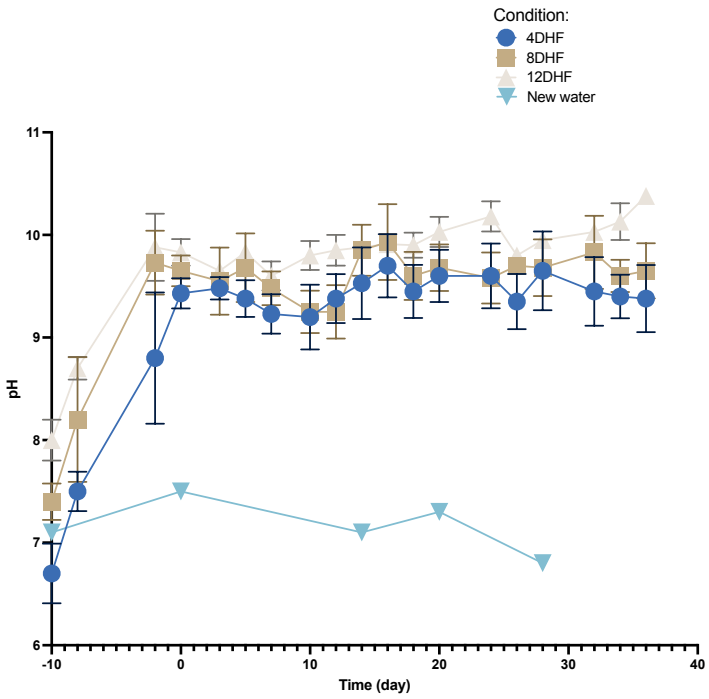

Figure E. 1: The measured pH values (means ± SD, n=3) for the three conditions in exp IV in addition to the pH of the new water added, in respect to time (day).

Appendix F: Total protein and total lipid for the individual harvestings

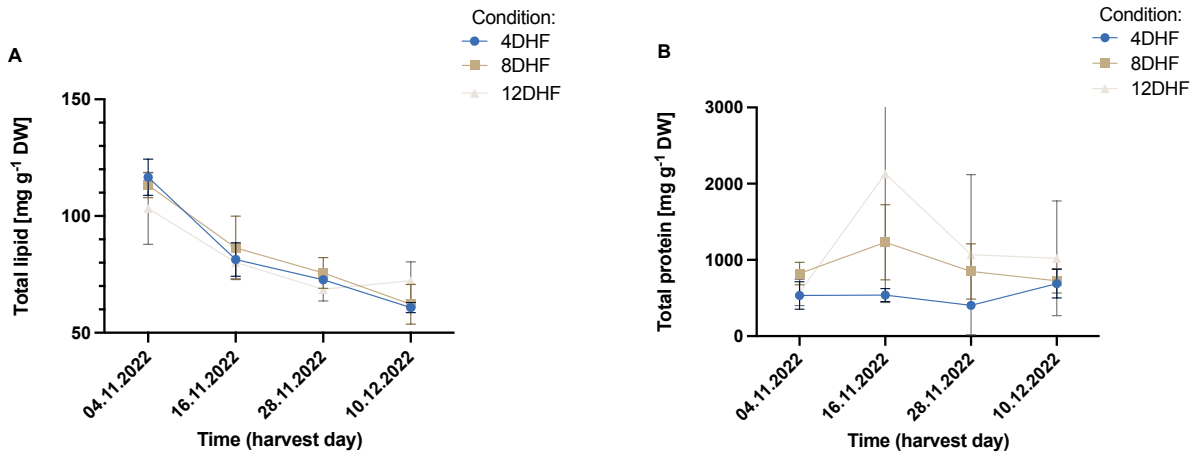

Figure F. 1: A: Total lipid (mg g^{-1} DW) (means ± SD, n=16) of the biofilm product in the three conditions, in respect to the four harvest days. **B:** Total protein (mg g^{-1} DW) (means ± SD, n=16) of the biofilm product in the three conditions, in respect to the four harvest days.

Appendix G: Microalgae biofilm formation process

Although the microalgal biofilm formation process is complex and species- dependent, the process can generally be described by dividing it into four main stages as shown in Figure G.1. The first step of the formation process is the reversible interaction between the microalgal cell membrane and the surface. This initial interaction needs to overcome the repulsive electrostatic interactions between the surface and the cell, and is dependent on two main factors; the chance of a cell to make direct contact with the surface and cell-surface interactions such as e.g. acid-base interactions or Van der Waals interactions (Zhuang et al., 2018, Stanley and Lazazzera, 2004, Hu et al., 2021). The second step is biofilm thickening, in which the microorganisms utilize the available nutrients and undergo division and complex biochemical processes, creating mature biofilm (Hu et al., 2021). As mentioned, unless grown under axenic conditions, microalgal biofilm is normally colonized by bacteria (Hu et al., 2021).

Bacterial cells and/or cells of other microorganisms will also adhere and form cell-cell interactions with the microalgae, creating a multispecies consortium where complex cross communication takes place (Liu et al., 2017, Wang et al., 2018). Microalgal cells can even produce transparent exopolymer particles (TEP), which are acidic sugar monomers and will attract bacterial cells, bringing crucial micronutrients to the biofilm environment (Cheah and Chan, 2021). Both bacterial and microalgal cells will start to produce EPS, which will create a net-like structure, providing the structure of the biofilm and strengthening the bonds between the cells. Thus, the cells are bound irreversibly to the surface of the substrate (Wang et al., 2018). The biofilm formation process will then enter the exponential growth and maturation phase, known as the third step (Wang et al., 2018). During this phase, complex interaction between the present cells occur; substrate exchange, horizontal gene transfer (HGT) and intense cell-cell interactions such as quorum sensing (QS) (Zhang et al., 2020). Through these complex interactions the species community is able to alter the curse of the biofilm development to best fit with the environment (Zhang et al., 2020).

As the biofilm thickens, nutrients and light will be more available at the surface of the film, resulting in the formation of different layers throughout the biofilm (Wang et al., 2018). Especially for multispecies biofilms, the different species may aggregate to form layers in locations in the biofilm where their specific needs are met (Wang et al., 2018). Cells located close to the surface are typically performing photosynthesis, while those in the deeper layers are typically heterotrophs (Hu et al., 2021). The fourth step is initiated when the biofilm has reached a mature state, generally characterized by being densely populated and able to retain nutrients in the EPS (Schnurr and Allen, 2015). While dispersion of biofilm may occur and regeneration of new biofilm is initiated, the biofilm is continuously adapting to best fit with its environment (Cheah and Chan, 2021, Liu et al., 2017).

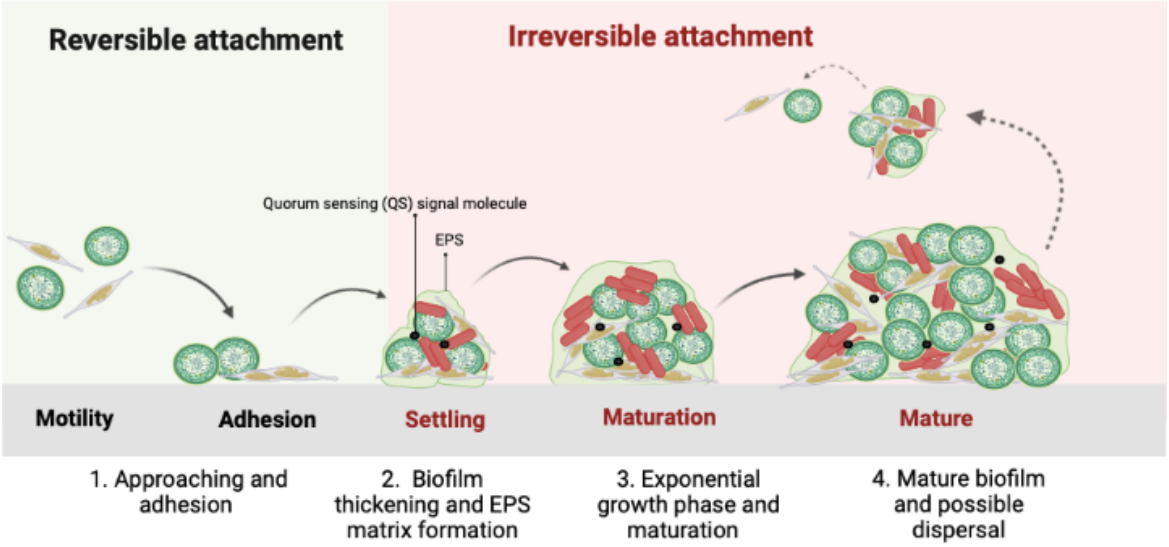

Figure G. 1: The process of microalgal biofilm formation can be described in general terms by dividing the process into four steps. (1) Free floating microalgal cells (here visualized as green microalgae and pennate diatom cells) interacts with surface, by overcoming the repulsive electrostatic interactions at the surface, and forming cell- surface interactions. (2) Microalgal cells, often alongside other microorganisms such as bacteria (here shown in red), will utilize available nutrients and undergo division, initiating the biofilm thickening. EPS will be secreted forming a net like structure, thus, causing an irreversible attachment. (3) During the exponential growth and maturation phase, complex interaction between the present microbial cells occurs, often resulting in different layers where specific activities are carried out or certain species are dominating. (4) The state of mature biofilm is reached, where nutrients are retained in the EPS. Dispersion of biofilm patches may occur. Illustration made using Biorender.

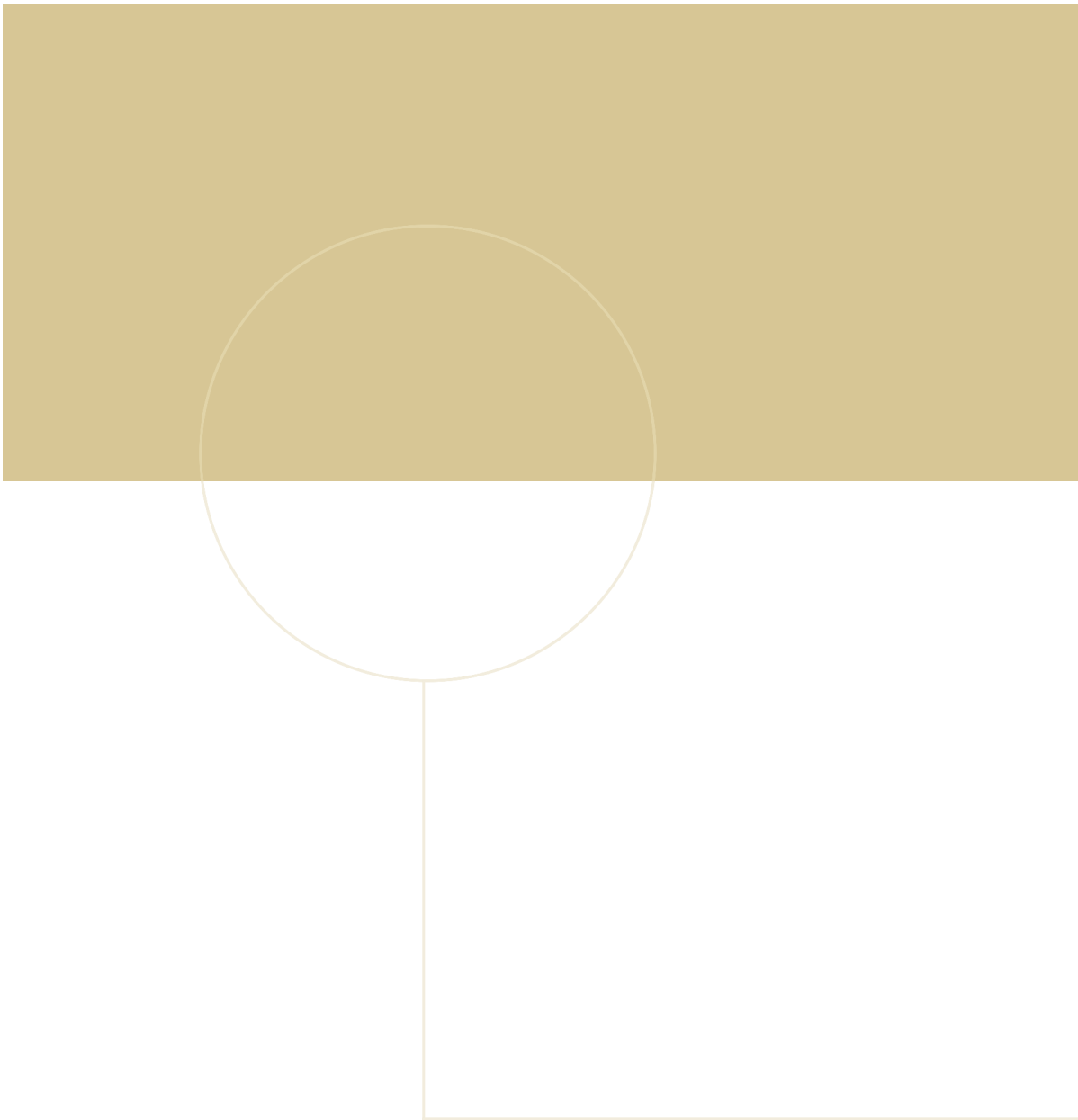

NTNU

Norwegian University of
Science and Technology